Satellite Detection of Air Pollution: Air Quality Impacts of Shale Gas Development in Pennsylvania

Preprint · May 2020

CITATIONS
0

READS
1,284

6 authors, including:

Ruohao Zhang
Centre College
10 PUBLICATIONS **5** CITATIONS
SEE PROFILE

Elaine Hill
University of Rochester
73 PUBLICATIONS **803** CITATIONS
SEE PROFILE

Satellite Detection of Air Pollution: Air Quality Impacts of Shale Gas Development in Pennsylvania

Ruohao Zhang[a,*], Huan Li[b], Neha Khanna[a],
Daniel M. Sullivan[c], Alan J. Krupnick[d], and Elaine L. Hill[e]

[a] *Department of Economics, Binghamton University, Binghamton, NY*
[b] *Department of Economics, North Carolina A&T State University, Greensboro, NC*
[c] *J.P. Morgan Chase, Washington DC.*
[d] *Resource for Future, Washington DC.*
[e] *Department of Public Health Sciences, University of Rochester, Rochester, NY*

This version: May 21, 2020

Abstract

This paper estimates the impact of shale gas development on local particulate matter pollution by exploiting a quasi-experimental setting in Pennsylvania where some wells experienced pre-production and/or production activities whereas some others were permitted but not spud between 2000 – 2018. We measure local PM pollution using daily aerosol optical depth (AOD) over a 3 kilometers circular area around every shale gas well. Using a spatial difference-in-differences model, we find that both shale gas pre-production and production activities increase daily AOD significantly, by 1.35% – 2.19% relative to the baseline. The effect of pre-production is slightly larger than production activities, but both effects attenuate with distance from the centroid well. Accounting for airborne spillovers, fracking increases AOD by 1.27% – 5.67%, which translates to $0.017\mu g/m^3$–$0.062\mu g/m^3$ increase in PM 2.5 concentration. This increase in PM 2.5 is associated with 20.11 additional deaths.

Key words: shale gas, particulate matter, aerosol optical depth, spatial DID, mortality impact

JEL codes: I15 I18 Q52 Q53 R11 R12

* Corresponding author. Tel. +1 (). E-mail: rzhang47@binghamton.edu.

1 Introduction

The United State's shale gas industry has developed rapidly in the past decades, growing from 1.6% of total natural gas production in 2000 to 69% in 2018 (Sieminski, 2014). The boom in shale gas production is largely due to the application of a new technology known as hydraulic fracturing. Recent work has shown that the hydraulic fracturing technology and its massive deployment impacts not only local economic but also local environmental conditions, including ground water contamination (Hill and Ma, 2017; Osborn et al., 2011; Jackson et al., 2013) and chemical exposures to surface water (Olmstead et al., 2013). In addition, various air pollutants including CO, NO_x, SO_x, particulate matter (PM), and volatile organic compounds (VOC) are released to the air from unconventional wells' preparation and fracking operations (Allen et al., 2014; Litovitz et al., 2013). However, the effects of shale gas development on local air pollution have not been evaluated.

We examine whether shale gas development in Pennsylvania has led to detectable changes in local PM pollution between 2000 and 2018 and the magnitude of those changes. Pennsylvania is the largest producer of shale gas among all states, and produces almost 30% of total shale gas in the whole country (EIA Website, 2019). Our particular focus on PM rather than the other types of air pollutants is important for two reasons: First, there is documented public concern that shale gas drilling activities contribute to local PM pollution (Litovitz et al., 2013), yet there is little causal evidence linking the two. Furthermore, while the literature has documented health effects on populations living close to unconventional wells (Currie et al., 2017; Hill, 2018), the channels explaining these effects are uncertain. PM pollution has known adverse health impacts (Atkinson et al., 2014), so understanding the causal effects of shale gas development on local PM pollution is relevant to policy.

Since the shale gas wells usually locate in the rural areas which are mostly not covered by the ground-based air quality monitors, we use a satellite based remote sensing data, daily Aerosol Optical Depth (AOD) data, as an indicator of PM concentration. AOD is a unit-less high-frequency and high-resolution measurement of PM concentration provided by specialized instruments on NASA's satellites. AOD measures the degree to which aerosols prevent the transmission of light by absorption or scattering of light through the entire vertical column of the atmosphere from the ground to the satellite sensors; therefore a higher value of AOD implies

higher concentration of PM pollution (Liu et al., 2004; Donkelaar et al., 2016). While the daily AOD captures the short-lived nature of the pollution (Sarigiannis et al., 2017), the measurment is sensitive to weather (Kumar et al., 2007; Foster et al., 2009). To solve this problem, we include as regressors a set of daily weather variables including precipitation, temperature, and dew point. We use AOD to estimate the pollution of shale gas industry, and covert the pollution in AOD to PM 2.5 using Lee et al. (2011)'s method for the purpose of estimating the mortality impact.

We define our study unit, named "Pollution area" (P-area), as a circular area of 3 kilometers radius around each unconventional well. The effect of wind on PM is captured econometrically, as detailed below. We expect that during the well pre-production phase, PM pollution will increase because well preparation activities, such as drilling and the associated commercial vehicle traffic, bring dust and diesel combustion to well sites and nearby roads. Similarly, we expect elevated PM pollution during gas production from on-site diesel combustion (Litovitz et al., 2013) and fugitive emissions.[1] Since the two periods may have different impacts on local PM pollution, we divide the life cycle of unconventional wells into three phases: inactive, pre-production, and production, and focus on the effects of the pre-production and production treatments on local PM pollution.

To estimate the causal effects of the two treatments on local PM pollution in the vicinity of hydraulically fractured wells, we need to construct the appropriate counterfactual. The Pennsylvania Department of Environmental Protection reports that not every well that is permitted eventually gets spudded and drilled (PA DEP Web, 2012). We use the PM pollution in the vicinity of these wells to construct the counterfactual because they are not associated with pre-production or production activities but are likely located in areas with similar geology and social-economic conditions as the wells that are spudded or producing. On the basis of this, we assign P-areas to the treatment group if their centroid wells have ever been in either the pre-production or production treatment, while P-areas are included in the control group if their centroid wells were permitted but never started the pre-production phase (i.e. not spudded). Such a quasi-experiment setting allows us identify the causal difference-in-differences estimates of the effect of the two treatments on local air quality in the vicinity of hydraulically fractured

[1] Fugitive emissions include benzene, toluene, ethyl-benzene, xylem other toxic hydrocarbons (Srebotnjak and Rotkin-Ellman, 2014). These aerosols can interact with sunlight and water vapor to form liquid particles, and are considered the secondary source of PM pollution.

wells.

It is important, however, to note that the estimation of the treatment effects is complicated by the potential "spillover" of one well's activities on its neighboring wells' P-areas. The spillover may arise from two channels. First, because PM pollution is air borne and travels with wind, a well's pre-production and production operations may increase PM pollution in downwind P-areas. Second, a cluster of wells may share infrastructure, such as road access to the fracking site, pipelines, waste pits, and other facilities needed for the fracking operation, thereby lowering the marginal change in PM pollution at a new well's P-area. To deal with the spatial spillover effects, we implement a spatial difference-in-differences model (Delgado and Florax, 2015), that allows the potential outcome of spatial units to be affected by not only their own treatment status, but also their neighboring units' treatment through spillovers. The model uses daily information on wind speed and direction to model the potential airborne spillovers from one well to another. We account for the second channel by including the number of wells in the pre-production phase, in production, or plugged in the 20 km radius around every well area as control variables in our regression.

Our data set includes all 20,677 unconventional wells in PA between February 24, 2000 and September 20, 2018. We have an unbalanced panel with 11,470 areas (17,506,147 area-day observations) in the treatment group and 9,207 areas (14,025,840 area-day observations) in the control group. Among the treatment group observations, we have 1,004,184 area-day observations in the pre-production phase and 3,607,236 area-day observations in the production period.

We find statistically detectable changes in daily AOD during both the pre-production and production phases of a marginal unconventional well. Not surprisingly, the marginal increase in AOD is higher during the pre-production phase (2.19% relative to the baseline AOD) than during production (1.35% of baseline). Furthermore, while the airborne spillover effects decline with distance from a centroid well, they can be felt not only within the P-area but also as far as 10 km downwind. Accounting for airborne spillovers, fracking increases AOD by 1.27% for the whole sample, and by 5.67% for the subsample of P-areas with a treated well. Based on Lee et al. (2011), these overall increases in AOD imply that daily PM concentrations increased by $0.017\mu g/m^3$ and $0.062\mu g/m^3$, respectively, in the average P-area. Using the concentration

response functions in Lepeule et al. (2012) and Fowlie et al. (2019), we estimate that this resulted in an additional 20 deaths between 2010 and 2017 in 671 census block groups (across 40 counties) which contains at least one shale gas well, with a total population of about 840,000 and an annual average death rate of 12 per 1000.

Our results are relevant for policy makers who seek to understand the welfare effect of shale gas development. They are also relevant for the communities located close to shale gas wells in terms of understanding the local air quality impact.

2 Link between Shale Gas Development and Local Air Pollution

2.1 The Link

The innovation of hydraulic fracturing and horizontal drilling technology decreased the production cost of shale gas significantly, making unconventional production economically feasible and boosting the size of the shale gas industry. The rapid expansion of natural gas development increased the supply of natural gas and lowered the prices relative to the scenario without hydraulic fracturing (Newell and Raimi, 2014). Abundant natural gas with relatively lower prices has facilitated the displacement of coal to natural gas in power plants, leading to air quality improvement. At the same time, relatively lower prices encourage more consumption of energy. Newell and Raimi (2014) show that the boom of shale gas development has reduced green house gas emissions in the US, which is driven by the fact that the retirement of coal-fired power plants dominates the effects of increased energy consumption.

Despite the positive global and regional environmental externality, the shale gas boom has raised concerns regarding *local* air quality because of the extensive activities associated with well preparation and gas production. Most fracking activities come with diesel combustion and dust, increasing emissions of ambient pollutants like CO, NO, hydrocarbons, PM, etc. It usually takes several months to complete well preparation (Hill, 2018). Activities include building roads, clearing sites, and transporting heavy equipment. Fracking requires a large amount of heavy equipment, such as drilling rigs, high-volume fracking pumps, and large size storage tanks, and this equipment typically arrives at the site on heavy trucks. According to Graham et al. (2015), it takes roughly 1,500 heavy-truck trips to deliver equipment and materials to a site and to remove the construction and drilling wastes from the site. In addition, off-road heavy-duty

engines are used to construct drill rigs and hydraulic fracturing pumps (Roy et al., 2014). When the construction is completed, a completion venting is performed for cleaning and bringing the well to production (Roy et al., 2014). The venting occurs multiple times during the whole life-cycle of an unconventional well as a maintenance procedure, and is known to be a major source of of volatile organic compounds (VOCs) emissions from unconventional wells.

During the production period, on-site equipment, including compressors to maintain the pressure of produced natural gas and other diesel machinery for well maintenance, result in diesel and natural gas combustion and air pollution. Additionally, when gas is flared, vented, or accidentally leaked during production, it also releases toxic air pollutants. Toxic air pollutants and VOCs including benzene, toluene, ethyl-benzene, xylem other toxic hydrocarbons come from direct and fugitive emissions of hydrocarbons at the well and from associated infrastructure such as condensate tanks (store liquid separated from produced natural gases), dehydrators (remove water from the produced natural gas), waste water impoundment pits, and pipelines (Srebotnjak and Rotkin-Ellman, 2014). In addition, many of these aerosols can interact with sunlight and water vapor to form liquid particles, and are considered a secondary source of PM pollution. In fact, secondary aerosols contribute a large portion of total PM, and are the dominating source of PM in many cases (Larsen et al., 2012; Heo et al., 2009; Lewandowski et al., 2008; Huang et al., 2014).

2.2 Local Air Pollution Measurements

Since many of the pollutants emitted during the well's pre-production and production phase are either primary or secondary sources of PM, we use PM to indicate the impact of shale gas development on local air quality. PM measurements are available from multiple sources, including the EPA's ground-based mobile monitoring, network stations, aircraft measurements, and a satellite platform as summarized in Field et al. (2014). Only the satellite platform provides a hyperlocal, daily measurement of PM. We therefore take advantage of NASA's satellite based measurements of aerosal optical depth (AOD), which is a high-frequency and high resolution (3 km $\times$ 3 km) measure, and is known to be one of the most robust aerosol parameters retrieved by the Moderate Resolution Imaging Spectroradiometer (MODIS) on NASA's satellites (Streets

et al., 2013).[2] [3]

More importantly, the literature has shown that AOD is a good predictor of PM of different sizes: $PM_{2.5}$ (size $< 2.5\mu m$) and PM_{10} (size $< 10\mu m$) (Liu et al., 2004; Donkelaar et al., 2016). Higher AOD indicates worse air quality, and therefore higher PM pollution. An advantage of using AOD is that it offers daily air quality observations with high geographical resolution. The spatial scale of the air pollution from shale gas wells is small. Companies conduct the drilling process on about a 3-acre pad of land, with a number of trucks that become part of an oil and gas drilling process. Given the sources of air pollution are from truck traffic and on-site construction and production process, we focus on a 3 km circular area around each single well.

Our use of AOD as a measure of air quality is not unique in the economics literature. Zou (2019) studies the current EPA policy of intermittent monitoring of environmental standards, and uses AOD to measure air quality when ground monitoring is off. His study finds air quality significantly worse on unmonitored days. Foster et al. (2009) studies the air pollution impact of a voluntary pollution reduction program in Mexico, and its consequence on infant health. They find a significant drop in AOD (increase in air quality) associated with the program, along with a significant drop in infant mortality due to respiratory illness associated with the decreasing in AOD. Sullivan and Krupnick (2019) uses AOD to measure the air quality in individual counties across the US, and argue that due to the limited number of ground monitors, many counties are mistakenly assigned as being in "attainment" with the 2015 National Ambient Air Quality Standards for PM. They estimate that 24.4 million people live in attainment areas that AOD data suggests should be in nonattainment. A similar result is also found by Fowlie et al. (2019).

3 Empirical Model

3.1 Estimating the Average Treatment Effects

Our baseline model follows a difference-in-differences framework:

$$q_{id} = \eta_c T^c_{id} + \eta_p T^p_{id} + \boldsymbol{A}_{id}{}'\Lambda + \boldsymbol{Z}_{id}{}'\zeta + \mu_i + \sigma_d + u_{id} \tag{1}$$

[2] There are two NASA satellites with MODIS instruments: Aqua and Terra. We use Terra because it has a longer observation period (start from Feb. 2000, whereas Aqua starts from May 2002).

[3] AOD is generated by the following method: the remote sensors record the interaction between electromagnetic radiation and aerosols including solid and liquid particles in the atmosphere, then convert the recorded results to AOD by applying the radioactive transfer models (Remer et al., 2005).

Here, q_{id} represents the AOD of P-area i on date d. T^c_{id} and T^p_{id} are treatment dummy variables, with $T^c_{id} = 1$ and $T^p_{id} = 1$ indicating the centroid well of P-area i is in the pre-production or production period respectively on date d, and zero otherwise. The two way fixed effects are P-area fixed effect μ_i and date fixed effect σ_d; thus in the difference-in-differences framework, η_c and η_c estimate the average treatment effects of the pre-production and production treatments, respectively.

$\boldsymbol{Z}'_{id}$ and $\boldsymbol{A}'_{id}$ are vectors of covariates. $\boldsymbol{Z}'_{id}$ contains four weather variables: precipitation, dew point, temperature, and wind speed. $\boldsymbol{A}'_{id}$ includes three additional variables to address the density of wells in the surrounding 20 km radius around every centroid well of P-area i. They are the daily counts of wells with pre-production, production, and inactive status.[4] Together, these variables account for the potential sharing of infrastructure, such as main roads, rigs and pipelines in the fracking area across wells. At the same time, the density of inactive wells – wells that used to be in the pre-production or production phase before date, but do not have on site activities anymore, reflects temporal variation in local geological conditions of shale gas stock that we expect is correlated with the productivity of wells in the area.

3.2 Estimating the Average Treatment Effects with Spatial Spillovers

Motivation: spillover path and quantification

PM travels with wind, bringing a well's pre-production and production treatment effects to downwind areas. This spillover effect would not be a concern for us if it affected the neighboring P-areas' air quality *randomly*. Non-randomness in wind blown spillover may arise from spatial segregation between treatment and control groups or temporal variation of wells' pre-production and production treatments.

Figure 1 shows the location of permitted wells in PA. While there is negligible regional segregation between treatment and control groups (see Figure 2 and 3), the temporal variation in the pre-production and production phases among wells (see Figure 4) suggests that the spillover effects might be nonrandom in our study setting.[5]

[4] Inactive wells are those wells that are without any operations.

[5] The pattern of nonrandom spatial and temporal spillovers is more clear in Table 1, *Panel II*. The summary statistics show that the densities of wells in the pre-production and production phases are much higher around treated group than control group.

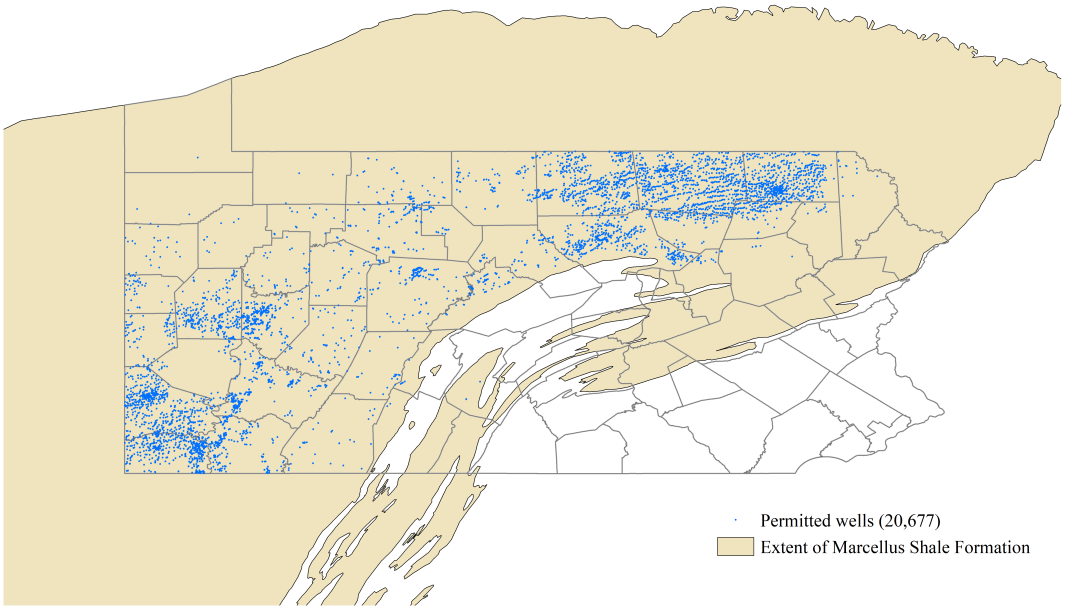

Figure 1: Permitted Wells in 2000 – 2018

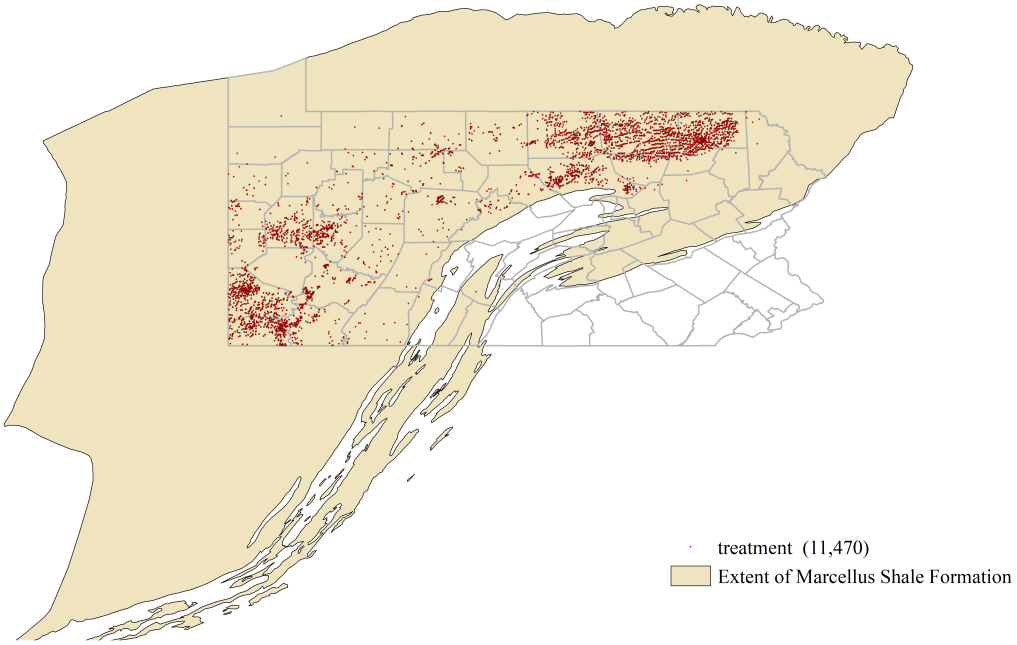

Figure 2: Wells in Treatment Group

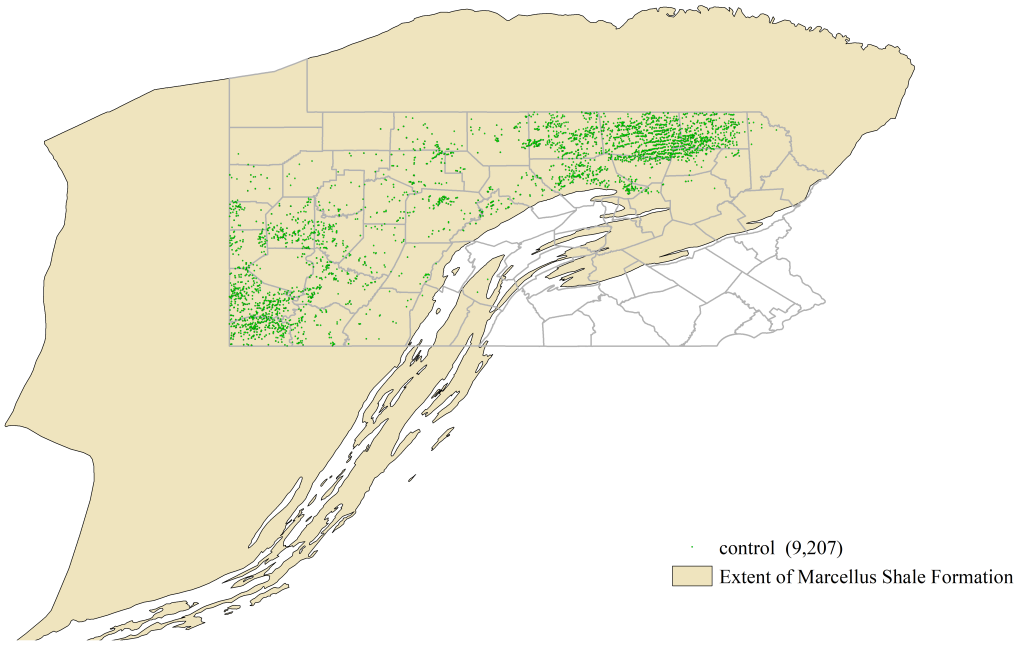

Figure 3: Wells in Control Group

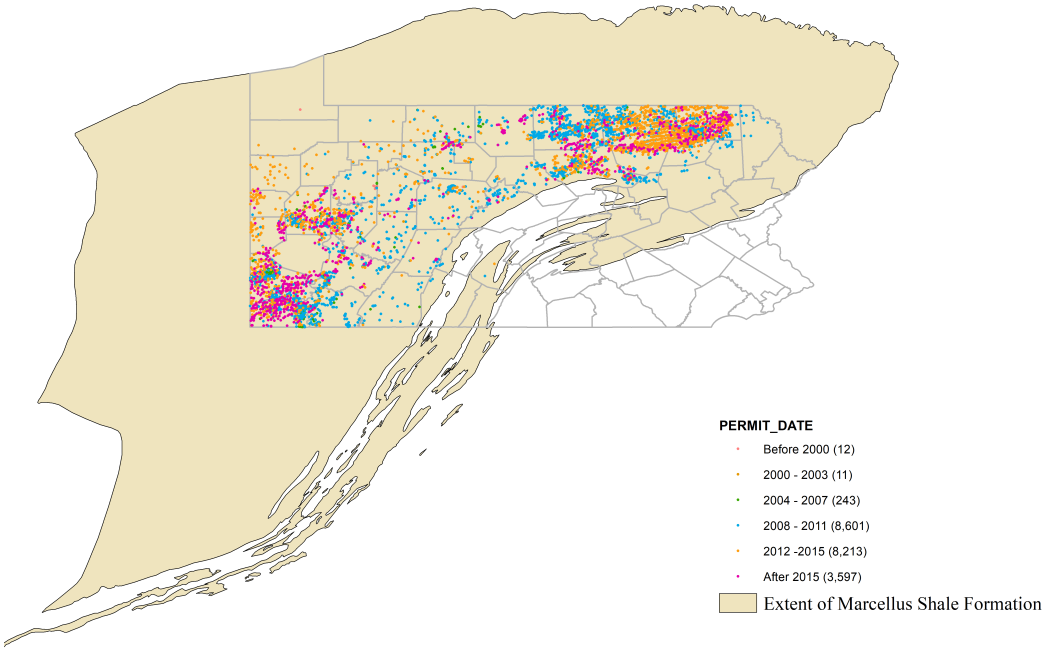

Figure 4: Well Location by Permit Years

We follow Delgado and Florax (2015)'s model to handle the nonrandom spatial spillover. Delgado and Florax (2015) account for a spatial spillover in potential outcome through a binary time-invariant spatial weight matrix, which equals 1 if the neighboring area is within a threshold

distance, and zero if not. In our setting, we expect the spillover effects through wind to attenuate by distance. Therefore, we distinguish 3 circular rings around each P-area's centroid well: 0–2 km, 2–5 km, and 5–10 km (hereafter referred to as bins), and allow the spillover effects from the upwind wells' pre-production and production activities to differ by bins. In addition to distance, wind direction matters too. The closer the wind direction to the geographic direction of the two wells, the stronger the spillover effects would be, conditional on the distance between the two wells. This can be addressed by the angle between any two wells' geographic direction and the wind direction. Therefore, our spatial weight matrix is continuous and various by date, because the wind direction is different every day.

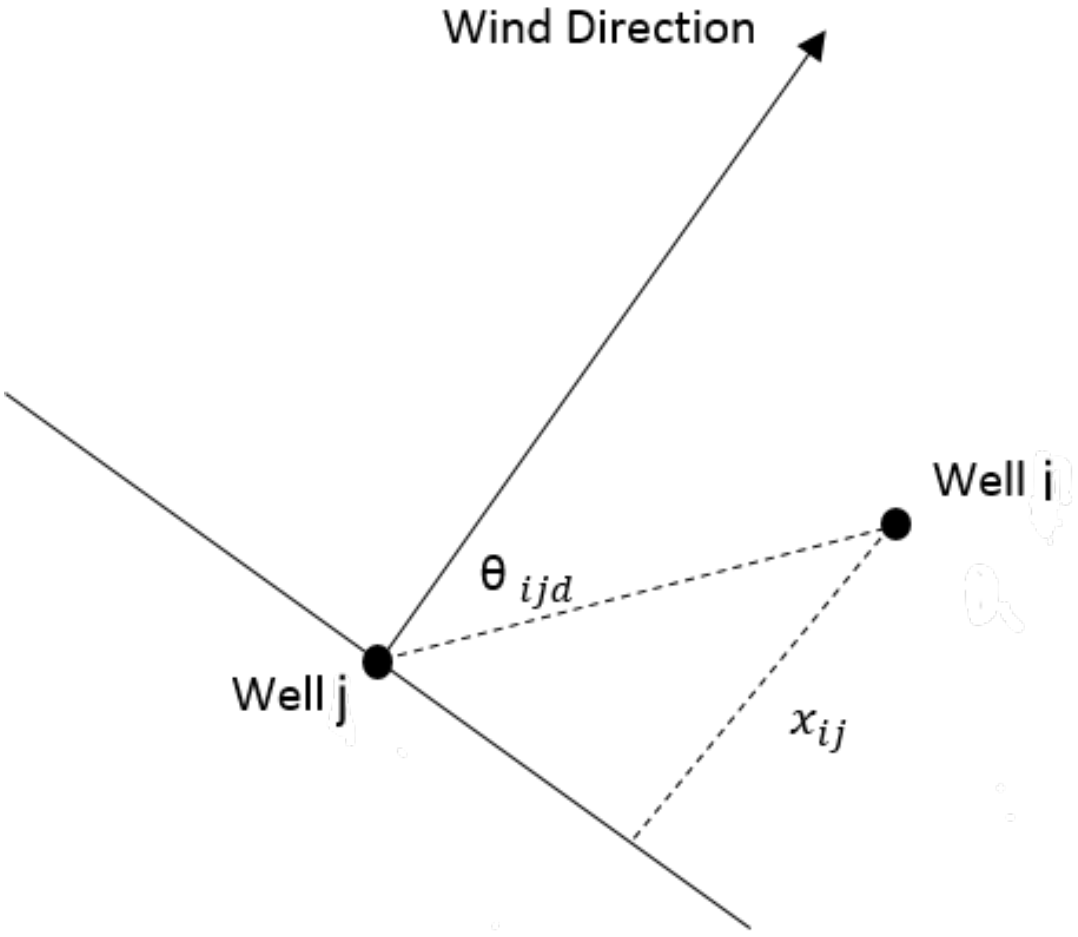

Figure 5: Pollution Transportation by Wind

Define $\boldsymbol{w}_{id}^{bin}$ as a $1 \times N$ matrix (spatial weight matrix) for the P-area with centroid well i on day d, where N is the total number of centroid wells (of both treatment group and control group P-areas) in our sample. The j^{th} element in $\boldsymbol{w}_{id}^{bin}$, indicated by w_{ijd}^{bin}, measures the magnitude

of the spillover effects that the P-area with centroid well i would receive from the well j in the bin bin on day d. We allow w_{ijd}^{bin} to vary over time depending on j^{th} well's treatment status on day d and whether it is located upwind of well i. To quantify w_{ijd}^{bin}, we use the two wells' geographical locations and wind direction on the day d. As shown in Figure 5, suppose θ_{ijd} is the angle between the wind direction and the geographical direction between the wells j and i on day d, and x_{ij} is the perpendiculars distance between the two wells. Then w_{ijd}^{bin} is defined as:

$$
\begin{aligned}
&w_{ijd}^{0-2} = cos(\theta_{ijd}) \text{ if } \theta_{ijd} \leq \pi \text{ and } 0 < x_{ij} \leq 2, \qquad w_{ijd}^{0-2} = 0 \text{ otherwise} \\
&w_{ijd}^{2-5} = cos(\theta_{ijd}) \text{ if } \theta_{ijd} \leq \pi \text{ and } 2 < x_{ij} \leq 5, \qquad w_{ijd}^{2-5} = 0 \text{ otherwise} \\
&w_{ijd}^{5-10} = cos(\theta_{ijd}) \text{ if } \theta_{ijd} \leq \pi \text{ and } 5 < x_{ij} \leq 10, \quad w_{ijd}^{5-10} = 0 \text{ otherwise}
\end{aligned}
$$

The definition of w_{ijd}^{bin} follows the spillover path: it implies that the weight is zero if the the well j is downwind of the P-area i, and the weight is positive if the the well j is located in the upwind of the P-area i. A smaller angle between the wind direction and the geographical direction from well j to P-area i means the treatments from well j has larger effect on P-area i. The design of spatial weight matrix follows the spirit of the Gaussian point source dispersion model[6], in which the aerosol travels along the downwind direction, and diffuses along the crosswind direction.

Model specification

In the light of Delgado and Florax (2015), we use the following spatial difference-in-differences model as our preferred benchmark model:

$$
\begin{aligned}
q_{id} =& \eta_c T_{id}^c + \eta_p T_{id}^p + \sum_{3bins} \beta^{bin,c} \boldsymbol{w}_{id}^{bin} \boldsymbol{H}_d^{bin,c} + \sum_{3bins} \beta^{bin,p} \boldsymbol{w}_{id}^{bin} \boldsymbol{H}_d^{bin,p} \\
&+ \boldsymbol{A}_{id}{}' \Lambda + \boldsymbol{Z}_{id}{}' \zeta + \mu_i + \sigma_d + u_{id}
\end{aligned} \tag{2}
$$

Where q_{id}, T_{id}^c, T_{id}^p, $\boldsymbol{A}_{id}'$, and $\boldsymbol{Z}_{id}'$ have the same definitions as in Equation (1).

$\boldsymbol{w}_{id}^{bin}$ is the spatial weight matrix, $\boldsymbol{H}_d^{bin,c}$ is a vector of dummies for all wells, in which an element is equal to 1 *if and only if* the well is in P-area i's bin and this well was in the pre-production phase on day d. In matrix notion, $\boldsymbol{w}_{id}^{bin} \boldsymbol{H}_d^{bin,c}$ is a weighted sum of all pre-production treatments belonging to a given bin bin for P-area i on day d, indicating the spillover effects of

[6] Gaussian point source dispersion model is a fundamental model in atmospheric science. See Wikipedia page.

pre-production treatment that P-area i received from the *bin* on day d. The interpretation can be generalized to the other 5 variables.

4 Data

We create a comprehensive data set that includes every well that was permitted in Pennsylvania between February 24, 2000 and September 20, 2018. Our data set includes detailed information on each well and daily information on air pollution and weather from multiple data sources.

4.1 Pennsylvania Shale Gas Data

Our shale gas well data is compiled from two sources published by Pennsylvania Department of Environmental Protection: "Oil Gas Locations – Unconventional" and "Oil & Gas Well Production Report". These sources include information submitted by well operators, as required by PA DEP (Regulation Code Section 78a.121). Both data sources contain a unique well identifier and well coordinates, allowing us to merge information across these sources.

For each well we have information on its geographic coordinates and permit date, regardless of whether the well is spudded or not. For wells that were drilled, we have current well status, along with spud date, production period, and completion date if already plugged. This information allows us to determine each well's activities on any given day. Given our focus on air quality, we consider three different phase in the life-cycle of a well: not yet spudded (or inactive), pre-production phase, and production phase.

In total, we obtained 20,677 unconventional wells that were permitted over our study period. As shown in Figure 1, most of these permitted wells are located in the northeastern corner PA (Susquehanna and Bradford counties) and southwestern corner (Washington and Greene counties). This is because the depth of Marcellus Shale base in these regions ranges from 5,000 to 8,500 feet, higher than other parts of Pennsylvania, suggesting that these areas are especially productive (PSU Web, 2009).

4.2 Local Air Quality: MODIS AOD

There are two NASA satellites with MODIS instruments: Aqua and Terra. We use the data provided by Terra because it has a longer observation period (starting from Feb. 2000, whereas

Aqua starts from May 2002). There are 4 levels of MODIS data available: L0 to L3. The higher level means the data is more pre-processed, but has lower spatial resolution. We use level 2 data[7] because it provides daily AOD observations at $3km \times 3km$ pixel resolution[8]. L2 data not only satisfies the requirements of our research design, but is also properly processed and can be directly used in our analysis.[9]

With the prior that the pre-production and production periods primarily affect local air quality, we define the P-area, our study unit, as an area surrounding a well with the $3km$ radius. There are two difficulties in determining a P-area's AOD (i) L2 AOD data is for $3km \times 3km$ square pixels, whereas P-areas are $3km$ radius circles. (ii) The pixels in the L2 data change every day according to the orbit of the satellite. We overcome these difficulties as follows: First we overlap all pixels with P-areas to find the square-circle intersections between pixels and every particular P-area for each day separately. Second, We assign every pixel a daily weight based on the daily intersection area to calculate the daily weighted average of AOD for each P-area.

For example, suppose on a day d, a P-area overlaps with pixel 1 and pixel 2 only. Pixel 1 has x_{1d} km^2 intersection area with P-area on day d and has AOD equals to q_{1d}. Pixel 2 has x_{2d} km^2 intersection area with P-area and AOD of q_{2d}. Then on day d the weight of pixel 1 is $\frac{x_{1d}}{x_{1d}+x_{2d}}$, and the weight of pixel 2 is $\frac{x_{2d}}{x_{1d}+x_{2d}}$. The weighted average AOD of P-area becomes $\frac{q_{1d}x_{1d}}{x_{1d}+x_{2d}} + \frac{q_{2d}x_{2d}}{x_{1d}+x_{2d}}$. In general, where a P-area overlaps with J pixels on day d, the weighted average AOD for P-area i is:

$$\begin{aligned}\text{AOD}_{id} =& q_{1d}\left(\frac{x_{1d}}{x_{1d}+x_{2d}+\cdots+x_{Jd}}\right)+\cdots+q_{jd}\left(\frac{x_{jd}}{x_{1d}+x_{2d}+\cdots+x_{Jd}}\right)\\ &+\cdots+q_{Jd}\left(\frac{x_{Jd}}{x_{1d}+x_{2d}+\cdots+x_{Jd}}\right)\end{aligned}$$

4.3 Weather

Our key control variables include daily information on local weather. We do so for three reasons: First, the weather variables account for the possible correlation between weather conditions and the choice of spud date. Second, the weather variables are important confounders of the strong

[7] We use version 6.1 MOD04_3K HDF data file. In the data file, we choose the layer "Corrected_Optical_Depth_Land".

[8] The level 2 data also provide $5km \times 5km$ resolution.

[9] L0 is raw spectral channel, and L1 is calibrated and geolocated radiance. Neither of them can be directly used. L3 also provide AOD , but the resolution becomes $1^\circ \times 1^\circ$ global grid, and the data is either 8 days or 1 month.

association between AOD and $PM_{2.5}$ (Kumar et al., 2007; Foster et al., 2009), and both pre-production and production activities affect AOD through $PM_{2.5}$. Third, wind information helps us address the spatial spillover, which occurs due to the spatial clustering of wells in PA.

The weather data is from the Parameter-elevation Regressions on Independent Slopes Model (PRISM), a spatial climate database. PRISM provides weather data including precipitation, mean temperature and mean dew point temperature at a daily frequency. One advantage of PRISM is that it is based on a spatial resolution of 4 km^2 pixels, which is comparable with the size of a well's P-area and the spatial resolution of AOD data. We process the daily precipitation, temperature and dew point data in a similar manner to the AOD data. That is, we overlay the 4 km^2 grid of weather data with P-areas and calculate the weighted average for each P-area using the (time-invariant) interaction areas as weights.

Daily information on wind speed and direction is from the National Centers for Environmental Prediction (NCEP)-U.S. Department of Energy Reanalysis II (NCEPRII). These daily data sets are available at resolution of 2.5 degree in latitude and longitude. We assign wind information to each P-area based on the 2.5 degree square that the centroid well is located in. Wind speed serves as an additional control variable, and wind direction is used to address the spatial spillover effects.[10]

5 Results

5.1 Model Estimation

Defining the Pre-production and Production Treatments

The duration of the two phases is unique to each well. Hence, we use each well's timeline: permit date, spud date, drilling and production phase, and plug date, to define its two treatments. Specifically, the first day of the pre-production phase is set either on the spud date or on the permit date, depending on which date is later.[11] Since the data sources do not report the

[10] The wind is decomposed into two component: U wind speed and V wind speed. U wind is the east-west component of wind. Positive U wind means the wind is from west to east, and negative U wind is from east to west. V wind is the north-south component of wind. Positive V wind means the wind is from south to north, and negative V wind is from north to south. The combination of U wind and V wind provides the wind direction and wind speed.

[11] In general, a well should be permitted before being spud, but there are few cases in which permit date was later than the spud date.

end of the pre-production phase, we set it as the day before the first day of production, under the assumption that wells start to produce immediately after the pre-production phase ends. See Appendix A.1 for additional details on how we use the production report to assign the pre-production and production treatment.

Clustered the Standard Error

When estimating the model, we cluster the standard errors by well pads. A well pad may consist of multiple wells, where P-areas frequently overlap. Yet, in our sample, 7,884 out of 20,677 unconventional wells do not have well pad information. We therefore assume that wells close to each other are located on the same well pad, and artificially assign the well pad ID to every individual well. In particular, any well that is closer than 63m to any other well is designated to be in the same well pad (Muehlenbachs et al., 2015). By comparing artificially designated well pad ID and original well pad ID if any, only 1.9% of wells with original well pad ID is mistakenly assigned into different artificial well pad.

5.2 Descriptive Statistics

The final sample is an unbalanced panel data consisting of 22,067 wells on 4,691 days, from February 24, 2000 – September 20, 2018. Out of the 22,067 permitted wells, 11,470 wells experienced pre-production or/and production phases and are included in the treatment group, the remaining 9,207 wells were not spudded and are included in the control group.[12] The majority of the wells in our sample were permitted after 2007 and are located in southwestern and northeaster corner of PA, as seen previously in Figure 4.

For the wells that have been spudded (i.e., wells in the treatment group), the pre-production phase lasts on average 406 days. Once the pre-production phase ends, wells produce for as long as 1,805 days (5 years), on average, until the production is completed. Table 1 presents summary statistics for our main analysis sample. We compare the mean statistics from the full sample and subsamples with treatment group observations in the pre-treatment period, pre-production period, production period, and control group observations separately. The mean daily AOD is 0.23 per P-area, with a standard deviation of 0.26. As shown in Table 1, through the whole

[12] In our data set, out of the 11,470 wells in the treatment group, 2,184 wells experienced pre-production phase only, 94 wells had information on production phase only, and 9,192 wells experienced both phases.

Table 1: Descriptive Statistics

Panel I: Key Variables

		Treated			
	Full Sample	Pre-Treatment	Construction	Production	Control
AOD	0.2275	0.2397	0.2005	0.1946	0.2267
	(0.2608)	(0.2726)	(0.2215)	(0.2160)	(0.2619)
Precipitation (mm)	1.2192	1.2141	1.1974	1.2287	1.2230
	(4.4304)	(4.4876)	(4.0946)	(4.2256)	(4.4521)
Temperature (Celsius)	12.3195	12.3527	12.0260	12.4069	12.2875
	(7.9863)	(7.8705)	(8.3065)	(8.3144)	(7.9817)
Dew Point (Celsius)	5.4960	5.4368	5.2807	5.7628	5.4972
	(8.5333)	(8.4274)	(8.7536)	(8.8462)	(8.5307)
Wind Speed (m/s)	3.9783	3.9655	3.9954	3.9791	3.9886
	(2.1202)	(2.1165)	(2.1345)	(2.1190)	(2.1230)

Panel II: Spillover Variables

		Treated			
	Full Sample	Pre-Treatment	Construction	Production	Control
Pre-production treatment	0.2227	0.1115	1.8842	0.3392	0.1760
in 0-2 km ring	(0.9799)	(0.6676)	(2.5011)	(1.2325)	(0.8339)
Pre-production treatment	0.7874	0.5145	2.7146	1.6458	0.6796
in 2-5 km ring	(2.3467)	(1.9266)	(4.1321)	(3.2900)	(2.1039)
Pre-production treatment	2.2152	1.4814	6.0632	4.6138	1.9974
in 5-10 km ring	(5.2077)	(4.3891)	(7.8726)	(6.8318)	(4.8720)
Production treatment	0.8618	0.2343	1.1749	3.8689	0.6429
in 0-2 km ring	(2.2909)	(1.1308)	(2.3953)	(3.9253)	(1.8729)
Production treatment	3.0912	1.1458	5.8850	11.5251	2.5108
in 2-5 km ring	(7.2320)	(4.2817)	(8.8516)	(11.4143)	(6.2403)
Production treatment	8.2211	3.3991	16.1812	27.5720	7.1076
in 5-10 km ring	(18.5921)	(11.5792)	(23.0690)	(28.6077)	(16.7869)
Density Pre-production	30.8528	20.2306	87.1349	62.1165	28.5484
(Number of wells, 20 km)	(50.6045)	(42.4766)	(63.8144)	56.6762	48.9225
Density Production	113.8012	47.4958	223.1352	363.2004	103.0471
(Number of wells, 20 km)	(203.3654)	(121.7000)	(226.0386)	(262.6684)	(192.5515)
Density Inactive	17.5413	7.4077	30.1685	54.2171	16.5211
(Number of wells, 20 km)	(35.1427)	(24.4105)	(36.2823)	(49.1666)	(32.5558)
Number of observations	31,531,987	12,894,727	1,004,184	3,607,236	14,025,840
Number of wells	20,677	11,470	11,376	9,286	9,207

AOD is missing for all observations receiving pre-production treatments with centroid well OBJECTID 383270. 107 wells are transformed from conventional to unconventional, their pre-production phases are not considered.

study period (Feb. 2000 – Sep. 2018), the treated areas' pre-treatment P-areas' average AOD is higher than control, but treated P-areas' average AOD is smaller. This might be explained by the combination of (i) the majority of wells were constructed and producing in later years and (ii) the AOD is declining over time in our sample, as shown in the first panel of Figure A1. The mean statistics of weather variables are relatively stable across full sample and subsamples. The rest of Figure A1 describes the yearly trend of weather variables.

In *Panel II* of Table 1, we summarizes the mean statistics of the spatial spillover variables. The non-random spatial clustering is clearly shown: subsample of pre-production observations has the largest mean values for the spatial spillover treatments of pre-production across all 3 distance bins as well as the highest density of wells in the pre-production phase in a 20km radius around centroid well. Likewise, the subsample of production observations has the largest mean value of spatial spillover treatments of production across all 3 distance bins as well as the highest density of wells under production in a 20km radius around centroid well. These statistics suggest the existence of the nonrandom spatial and temporal spillovers. We also find the subsample of production observations has a higher average density of inactive wells than the other samples.

5.3 Testing the Common Trend Assumption

The validity of our difference-in-differences estimation depends on the credibility of our control group P-areas to provide a reliable counterfactual. One way to assess the credibility is to test if the treatment and control groups share a common trend prior to the occurrence of the treatment. To test common trend assumption, we compare the daily differences between pre-treatment observations from the treated group and their corresponding control group observations on the same dates. Because we have staggered treatments on a large number of treated P-areas, the pre-treatment observations from the treated group covers all dates of our sample period, so all control observations are used in the test. We take a subset of data that consists of pre-treatment observations for treated P-areas and all observations for control group P-areas, and estimate the following model:

$$q_{id} = \boldsymbol{A}_{id}'\Lambda + \boldsymbol{Z}_{id}'\zeta + \mu_i + \sigma_d + \sigma_d \times T_i + u_{id}, \tag{3}$$

where T_i is the group fixed effect, with $T_i = 1$ indicating P-area i is in the treated group (i.e., pre-production or production), and $T_i = 0$ indicating P-area i is in the control group. σ_d is the day dummies. The coefficients on the interaction term $\sigma_d \times T_i$ capture the difference in the time trend in AOD between the treated and control groups. Standard errors are clustered by pad. Under the null hypothesis of a common trend, the coefficients on $\sigma_d \times T_i$ are insignificant. Rejecting the null hypothesis implies the absence of the common trend of AOD between the two groups.

Figure A2 shows the estimated coefficients of $\sigma_d \times T_i$ along with 99% confidence intervals. Because 87% of the coefficients are not significantly different from zero, we conclude that the pre-treatment trends in AOD in both groups are similar, and thus the P-areas with permitted but not spudded centroid wells serve as a suitable control group, providing us an appropriate counterfactual for pollution in the absence of shale gas development.

5.4 Main Results

Table 2 summarizes the average treatment effect of each P-area's own centroid well. Our baseline DID model shows that, on average, a P-area's AOD increases significantly when its centroid well is in pre-production and production. However, the estimates confound the effect due to wind blown pollution from upwind wells. Hence, our preferred benchmark estimates is based on the spatial DID model. Similar to the baseline DID model, the spatial DID model also shows that a well's pre-production and production activities significantly increase the daily AOD in its P-area. In terms of the magnitudes, the baseline model overestimates the treatment effect, possibly because there is temporally non-random variation of pre-production and production activities (see Figure 4), and the coefficients pick up the non-random airborne spillovers. According to the results from the spatial DID model, pre-production activity significantly increases a well's P-area AOD by 0.00429, which is 2.19% relative to the average AOD in our sample. Similarly, a well's production activities significantly increases AOD in its P-area by 1.35%. At the same time, we find that a well's pre-production activities increase its P-area's AOD more than the production activities. Our results are similar in magnitude to Zou (2019), who found a 1.6%-1.8% increasing in AOD when the ground PM monitor is off.

The results from the spatial DID model show that the spillover effects from wells in upwind

areas increase local AOD. Furthermore, while this effects attenuates by distance, both for pre-production and production treatments, it is statistically detectable at least as far as 10km from its emission source. Additionally, pre-production activities from upwind wells have a larger spillover effect than production activities in all the three distance rings.

5.5 Overall AOD Impact of Shale Gas Industry

We use the estimates reported in Table 2 to estimate overall increasing in AOD in each P-area due to unconventional shale gas development. Let the overall AOD increases in P-area i on date d be s_{id}, then

$$\hat{s}_{id} = \hat{\eta}_c T^c_{id} + \hat{\eta}_p T^p_{id} + \sum_{3bins} \hat{\beta}^{bin,c} \boldsymbol{w}^{bin}_{id} \boldsymbol{H}^{bin,c}_{d} + \sum_{3bins} \hat{\beta}^{bin,p} \boldsymbol{w}^{bin}_{id} \boldsymbol{H}^{bin,p}_{d}. \tag{4}$$

$\hat{\eta}_c$, $\hat{\eta}_p$, $\hat{\beta}^{bin,c}$ and $\hat{\beta}^{bin,p}$ are estimated coefficients from our main result shown in the last column of Table 2. We find that the overall effect of fracking increases AOD by 0.00276 for the whole sample, and 0.01031 for the subsample of observations under treatment. This represents a 1.27% and 5.67% increase in AOD above the background level which we estimate as $\hat{b}_{id} = q_{id} - \hat{s}_{id}$, where q_{id} is the observed AOD level.[13]

6 Robustness Checks

To evaluate the validity and robustness of the causal effects found in our main analysis, we conduct several additional analyse. First, we consider the fact that unobserved confounders such as the local communities' preferences and bargaining power in leasing land to the shale gas industry that correlate with both well location and social-economic conditions, so local air quality may lead to non-random sorting of wells into treatment and control groups. To address this, we consider three different subsamples: one includes wells from the treatment group only, and the other two use two different matching criteria. Second, considering the uncertainty regarding the start and end of the pre-production phase due to data limitations, we use two alternative pre-production phase definitions. Finally, we conduct two falsification tests. All of these sensitivity analyses support the average treatment affects in our main analysis.

[13]The percentage estimation is calculated by $\hat{s}_{id}/\hat{b}_{id}$.

Table 2: Summary results of average treatment effects: main analysis

	DID		Spatial DID	
Treatments	Coefficient	Std. Err.	Coefficient	Std. Err.
Own Effects				
Pre-production treatment	0.00624***	(0.00040)	0.00429***	(0.00039)
Production treatment	0.00463***	(0.00040)	0.00258***	(0.00036)
Spillover Effects				
Pre-production treatments in 0–2 km ring			0.00101***	(0.00010)
Pre-production treatments in 2–5 km ring			0.00050***	(0.00004)
Pre-production treatments in 5–10 km ring			0.00008***	(0.00002)
Production treatments in 0–2 km ring			0.00066***	(0.00008)
Production treatments in 2–5 km ring			0.00026***	(0.00003)
Production treatments in 5–10 km ring			0.00002***	(0.00001)
Control Variables				
Weather, well densities in 20km circular area, Two-way FEs	Y		Y	
Adjusted R^2	0.76		0.76	
Sample Size	31,531,987		31,531,987	

Note: The full results are reported in Appendix Table A3. The daily weather controls are mean precipitation, mean dew point, mean temperate and wind speed. The 20 km circular background condition include numbers of wells of three different operation status: pre-production, production, and inactive. Standard errors are clustered by well pads.

6.1 Using Treatment Group Only

Each well in the treatment group began pre-production or production phases at a different point in time, staggering the treatments in our sample. As Goodman-Bacon (2018) and Athey and Imbens (2018) have discussed, not only observations in the control group, but treatment group observations during the pre-treatment period and post-treatment period can also provide a valid counterfactual. For the sake of eliminating any confounding unobserved factors, we re-estimate the standard and spatial difference-in-differences models using a subsample of P-areas from the treatment group only.

The average treatment effects are reported in Table 3 are highly consistent with the main results: pre-production treatment and production treatment increase the AOD significantly; pre-production increases AOD more than production activities; and spillover effects from upwind wells' pre-production and production operations are significant and attenuate with distance. The magnitudes of the estimated coefficients are comparable to these in Table 2.

Table 3: Robustness check: using treatment group P-areas only

	DID		Spatial DID	
Treatments	Coefficient	Std. Err.	Coefficient	Std. Err.
Own Effects				
Pre-production treatment	0.00651***	(0.00040)	0.00475***	(0.00040)
Production treatment	0.00488***	(0.00060)	0.00281***	(0.00059)
Spillover Effects				
Pre-production treatments in 0–2 km ring			0.00086***	(0.00010)
Pre-production treatments in 2–5 km ring			0.00048***	(0.00004)
Pre-production treatments in 5–10 km ring			0.00008***	(0.00002)
Production treatments in 0–2 km ring			0.00060***	(0.00009)
Production treatments in 2–5 km ring			0.00025***	(0.00003)
Production treatments in 5–10 km ring			0.00003***	(0.00001)
Control Variables				
Weather, well densities in 20km circular area, Two-way FEs	Y		Y	
Adjusted R^2	0.76		0.76	
Sample Size	17,506,147		17,506,147	

Note: The full results are reported in Appendix Table A4. The weather controls are daily mean precipitation, daily mean dew point, daily mean temperate, wind speed. The 20 km circular background condition include numbers of wells of three different operation status: pre-production, production, and inactive. Standard errors are clustered by well pads.

6.2 Using Matched Samples

Figure 4 suggests non-randomness of the treatment across locations and permit issue dates. For example, there is a cluster of wells in the northeastern part of PA receiving permit during 2012–2015, whereas there is another cluster of wells in the southwestern part receiving permit after 2015. We trim this sample using two matching strategies to eliminate possible systematic differences driven by such non-randomness. In both matching strategies, wells in the control group are used repeatedly. The first strategy uses one-to-one matching by distance, permit year, and permit month. That is, each P-area in the treatment group is matched with the closest P-area in the control group, such that the centroid wells from the two P-areas are permitted in the same month and same year. The second strategy is one-to-one matching by distance, permit year, and county. In this case, each P-area in the treatment group is matched with its closest P-area in the control group from the same county, and the centroid wells of the two P-areas were permitted in the same year. These two matching strategies allow us to exclude control group observations from P-areas that are temporally and geographically distant from the regional clusters in the treatment group, so as to obtain a potentially more reliable counterfactual.

The first matching strategy gives us 11,368 wells in the treatment group and 3,000 wells in the control group. The average distance between a matched treatment P-area and a control P-area is 16.43 KM. The second matching strategy gives us 11,293 wells in the treatment group and 2,833 wells in the control group. The average distance between the matched treatment P-area and control P-area is 3.45 KM. For both subsamples, we find that the AOD balance is slightly improved, with the difference in the average AOD between the pre-treatment observations and control observations reduced from 0.013 to about 0.011. Figure A3 and Figure A4 demonstrate the locations of the wells in two matched subsamples. Using the two matched subsamples, we re-run the DID and spatial DID model, with the results reported in Table 4. The results are remarkably consistent with the main findings reported in Table 2.

Table 4: Robustness check: using matched samples

	Matched sample 1		Matched sample 2	
	DID	Spatial DID	DID	Spatial DID
Own Effects				
Pre-production treatment	0.00609***	0.00436***	0.00624***	0.00452***
	(0.00039)	(0.00038)	(0.00039)	(0.00038)
Production treatment	0.00449***	0.00262***	0.00475***	0.000291***
	(0.00051)	(0.00048)	(0.00051)	(0.00049)
Spillover Effects				
Pre-production treatments in 0–2 km ring		0.00093***		0.00093***
		(0.00010)		(0.00010)
Pre-production treatments in 2–5 km ring		0.00043***		0.00048***
		(0.00004)		(0.00004)
Pre-production treatments in 5–10 km ring		0.00008***		0.00008***
		(0.00002)		(0.00002)
Production treatments in 0–2 km ring		0.00061***		0.00060***
		(0.00008)		(0.00009)
Production treatments in 2–5 km ring		0.00026***		0.00027***
		(0.00003)		(0.00003)
Production treatments in 5–10 km ring		0.00002***		0.00002***
		(0.00001)		(0.00001)
Control Variables				
Weather, well densities in 20km circular area, Two-way FEs	Y		Y	
Adjusted R^2	0.76	0.76	0.76	0.76
Sample Size	21,949,389	21,949,389	21,583,079	21,583,079

Note: The full results are reported in Appendix Table A5 and Table A6. The weather controls are daily mean precipitation, daily mean dew point, daily mean temperate, wind speed. The 20 km circular background condition include numbers of wells of three different operation status: pre-production, production, and inactive. Standard errors are clustered by well pads.

6.3 Using Extended Pre-production Phase

In the main analysis, we assume that pre-production operations start on the spud date. But, the activities associated with pre-production phase might begin before the spud date. For example, building roads for accessing the well site and delivering equipment to the well site takes several weeks (Hill, 2018), both of which usually take place before spudding a well. Taking this into consideration, we extend the pre-production phase by one week and one month before the spud date, respectively, and re-estimate our model under these new definitions of the pre-production treatment.

Table 5 reports the results. The results of both baseline DID and spatial DID are not sensitive to the change of pre-production phase length. These results suggest the possibility that some pre-production activities may have commenced months before spud date, but the accuracy of our results stands.

Table 5: Robustness check: spatial DID using extended pre-production phase

	Extended by 7 days		Extended by 30 days	
	DID	Spatial DID	DID	Spatial DID
Own Effects				
Extended pre-production treatment	0.00626***	0.00434***	0.00620***	0.00433***
	(0.00040)	(0.00039)	(0.00039)	(0.00038)
Production treatment	0.00466***	0.00260***	0.00470***	0.00264***
	(0.00049)	(0.00046)	(0.00049)	(0.00046)
Spillover Effects				
Pre-production treatments in 0–2 km ring		0.00101***		0.00101***
		(0.00010)		(0.00010)
Pre-production treatments in 2–5 km ring		0.00050***		0.00050***
		(0.00004)		(0.00004)
Pre-production treatments in 5–10 km ring		0.00008***		0.00008***
		(0.00002)		(0.00002)
Production treatments in 0–2 km ring		0.00066***		0.00066***
		(0.00008)		(0.00008)
Production treatments in 2–5 km ring		0.00026***		0.00026***
		(0.00003)		(0.00003)
Production treatments in 5–10 km ring		0.00002**		0.00002**
		(0.00001)		(0.00001)
Control Variables				
Weather, well densities in 20km circular area, Two-way FEs	Y	Y	Y	Y
Adjusted R^2	0.76	0.76	0.76	0.76
Sample Size	31,531,987	31,531,987	31,531,987	31,531,987

Note: The full results are reported in Appendix Table A7.

6.4 Falsification Test

To validate the causal nature of our estimates, we implement falsification tests by excluding observations with true treatments and assigning placebo treatments on alternative days. We consider 2 placebo tests with arbitrary placebo treatments: in the first placebo test, we assign a placebo treatment from 1,080 days (about 3 years) before the pre-production phase to 720 days (about 2 years) before pre-production phase. In the second placebo test, we assign a placebo treatment from 1,440 days (about 4 years) before the pre-production phase to 1,080 days (about 3 years) before the pre-production phase. We assign a single placebo treatment for each test and do not distinguish between placebo pre-production and placebo production treatments.

The results are reported in Table 6: the coefficients on the placebo treatments are statistically insignificant, while the true spillover effects remains positive and significant. Thus, our results survive the two falsification tests, showing little evidence that the true treatments effect are distorted by AOD trends in the pre-treatment period.

Table 6: Robustness check: falsification tests

	Placebo Test 1		Placebo Test 2	
	DID	Spatial DID	DID	Spatial DID
Placebo Treatment	0.00019	0.00036	-0.00015	0.00008
	(0.00034)	(0.00033)	(0.00034)	(0.00034)
True Spillover Effects				
Pre-production treatments in 0–2 km ring		0.00120***		0.00119***
		(0.00012)		(0.00012)
Pre-production treatments in 2–5 km ring		0.00055***		0.00055***
		(0.00005)		(0.00005)
Pre-production treatments in 5–10 km ring		0.00013***		0.00013***
		(0.00002)		(0.00002)
Production treatments in 0–2 km ring		0.00070***		0.00070***
		(0.00010)		(0.00010)
Production treatments in 2–5 km ring		0.00029***		0.00029***
		(0.00004)		(0.00004)
Production treatments in 5–10 km ring		0.00002*		0.00002*
		(0.00001)		(0.00001)
Control Variables				
Weather, well densities in 20km circular area, Two-way FEs	Y	Y	Y	Y
Adjusted R^2	0.76	0.77	0.76	0.77
Sample Size	26,920,567	26,920,567	26,920,567	26,920,567

Note: The full results are reported in Appendix Table A8. Standard errors are clustered by well pads.

7 Welfare Analysis

Is the estimated increase in AOD due to shale gas development economically meaningful? To answer this question, we use a concentration response function to estimate the increase in mortality due to the increase in local PM pollution associated with the overall increase in AOD due to the shale gas development.

7.1 Convert AOD to PM 2.5

Epidemiological concentration response functions describe the magnitude of a population level health response from exposure to pollution. A first step in applying a concentration response function is to translate the change in AOD to a change in PM 2.5 concentration. To do this, we utilize the random coefficient model proposed by Lee et al. (2011). To predict the daily PM 2.5 concentrations for each P-area[14], we use daily PM 2.5 concentration data from all 41 monitors located in Pennsylvania to estimate the random coefficient model, and then use the estimated coefficients to predict the daily change in PM 2.5 concentration for each P-area due to fracking activities. Specifically, we estimate the following regression:

$$PM_{jd} = (\alpha + u_d) + (\beta + v_d)q_{jd} + m_j + \epsilon_{jt}, \tag{5}$$

where j denotes the monitor site, and d denotes date. q_{jd} is the average AOD value in a 3KM radius area surrounding each PM 2.5 monitor. m_j is the monitor specific random intercept, u_d is the date specific random intercept, and v_d is the daily random component in the slope of AOD. We assume $m_j \sim N(0, \sigma_m^2)$, $(u_d, v_d) \sim N((0,0), \Sigma)$, and

$$\Sigma = \begin{bmatrix} \sigma_u^2 & \sigma_u\sigma_v \\ \sigma_u\sigma_v & \sigma_v^2 \end{bmatrix},$$

and estimate equation 5 using maximum likelihood. Figure A5 shows that the predicted PM 2.5 concentration fits the true PM 2.5 concentration in the vicinity of ground monitors with $R^2 = 0.78$. Let $\hat{\alpha}$ and $\hat{\beta}$ be the estimated coefficients, let $\hat{u}_d$ and $\hat{v}_d$ be the daily value of random components. Recall that the background AOD impact is $\hat{b}_{it} = q_{id} - \hat{s_{id}}$, where q_{id} is the observed

[14] We do not observe daily PM 2.5 concentration on a fine geographic scale. This is our original motivation for using satellite-based AOD data rather than ground level measures of PM 2.5 concentration.

AOD, and $\hat{s_{id}}$ is the estimated AOD impact due to the shale gas development. The estimated PM 2.5 concentration and ambient/background PM 2.5 concentration can be represented by

$$\widehat{PM2.5}_{id} = \hat{\alpha} + \hat{u}_d + (\hat{\beta} + \hat{v}_d)q_{id} + \hat{m}_i, \tag{6}$$

$$\widetilde{PM2.5}_{id} = \hat{\alpha} + \hat{u}_d + (\hat{\beta} + \hat{v}_d)\hat{b}_{id} + \hat{m}_i. \tag{7}$$

where i is the P-area index and d is the date index. q_{id} is the observed AOD, and $\hat{m}_i$ is the estimated random intercept of each P-area. Then, the daily change in PM2.5 concentration due to shale gas development $\Delta\widehat{PM2.5}_{id}$ is estimated as

$$\Delta\widehat{PM2.5}_{id} = \widehat{PM2.5}_{id} - \widetilde{PM2.5}_{id} = (\hat{\beta} + \hat{v}_d)\hat{s}_{id}. \tag{8}$$

We find that on average, shale gas development increases the daily PM concentration by $0.017mg/m^3$ for the whole sample, and $0.062mg/m^3$ for the P-areas in the treatment group.

7.2 Mortality Impact

We estimate the change in mortality rates due to the estimated change in PM 2.5 concentration at the census block group level by year. We obtain the mortality data from CDC WONDER at the county level, which is the finest spatial resolution at which mortality data are available to the public. We obtain population data from the American Community Survey at the census block group level. Let the mortality rate for census block group k in year t be λ_{kt}. We assume that mortality is uniformly distributed across census block groups within a county, so $\lambda_{k't} = \lambda_{k''t}$ if census block group k' and k'' are in the same county. Let the impact in PM 2.5 concentration of shale gas development on census block group k be $\Delta\overline{PM2.5}_{kt}$. We approximate $\Delta\overline{PM2.5}_{kt}$ by averaging the yearly average overall impact in PM 2.5 concentration of P-areas whose centroid wells are located in census block group k. That is, $\Delta\overline{PM2.5}_{kt} = \frac{1}{N_{kt}}\sum_{i\in I_k, d\in t}\Delta\widehat{PM2.5}_{id}$, where N_{kt} is the total number of centroid wells in census block k and date in year t ($i \in I_k$ and $d \in t$).

(Krewski et al., 2009; Lepeule et al., 2012) estimate mortality concentration-response functions for PM 2.5 concentration. They utilize a Cox proportional-hazard model with log-linear functional form, which is also used by the EPA for Regulatory Impact Analysis (Fowlie et al.,

Table 7: Mortality Impact, 671 census block group containing P-areas

Year	Cardio	COPD	All Death	Population
2010	0.69 (3,104.83)	0.09 (555.43)	1.22 (9,522.19)	841,848
2011	1.16 (3,084.53)	0.15 (568.97)	2.10 (9,765.50)	845,607
2012	1.32 (3,022.89)	0.17 (543.39)	2.42 (9,670.84)	843,169
2013	1.11 (3,090.76)	0.15 (579.48)	2.04 (9,912.32)	845,133
2014	1.35 (3,053.58)	0.18 (555.91)	2.53 (9,866.78)	843,801
2015	1.96 (3,122.42)	0.28 (589.06)	3.70 (10,159.49)	838,444
2016	1.48 (3,111.75)	0.19 (553.01)	2.73 (10,074.72)	833,749
2017	1.78 (3,133.03)	0.23 (592.83)	3.36 (10,488.52)	828,150
Total	10.85 (24,723.80)	1.44 (4,538.08)	20.11 (79,420)	

Numbers in parentheses describe the death count.

2019). We use the same method to estimate the impact in mortality rate:

$$\Delta Deaths_{kt} = Pop_{kt}\lambda_{kt}\big(1 - exp(-\hat{\gamma}\Delta\overline{PM2.5}_{kt})\big), \tag{9}$$

where $\hat{\gamma}$ is the proportional hazard coefficient estimated by Lepeule et al. (2012), and Pop_{kt} is the block group k's population in year t. Appendix A.8 shows the detailed derivation of Equation 9.

Following previous studies, we estimate mortality due to all causes, cardiovascular disease, and chronic obstructive pulmonary disease (COPD). Let $\hat{\gamma}_{ALL}$, $\hat{\gamma}_{CARD}$, and $\hat{\gamma}_{COPD}$ be the estimated coefficient of the proportional hazard coefficients. Lepeule et al. (2012)'s study suggests that for every 1 ug/m^3 increment in PM 2.5 concentration, $\hat{\gamma}_{ALL} = 0.0131$, $\hat{\gamma}_{CARD} = 0.0231$, and $\hat{\gamma}_{COPD} = 0.0157$. Table 7 reports the estimated impact on mortality of the shale gas industry through PM 2.5 pollution for 671 census block groups in Pennsylvania where unconventional wells are located. Table 8 reports the estimated impact on mortality of all causes in top 4 counties in terms of the numbers of active shale gas wells. Our results suggest that from 2010 to 2017, shale gas development caused an additional 20.11 deaths in a population of 840,000 through PM

Table 8: Mortality Impact of All Death, counties with most P-areas with active wells

Year	Washington	Susquehanna	Bradford	Greene
2010	0.28 (1,043.55)	0.05 (343.67)	0.11 (440.22)	0.10 (377.18)
2011	0.40 (1,085.06)	0.12 (354.03)	0.22 (436.16)	0.16 (351.16)
2012	0.43 (1,085.50)	0.14 (316.28)	0.20 (416.10)	0.18 (367.02)
2013	0.39 (1,101.69)	0.13 (347.16)	0.14 (453.45)	0.17 (354.29)
2014	0.50 (1,096.74)	0.18 (377.50)	0.15 (467.68)	0.22 (319.16)
2015	0.78 (1,133.99)	0.32 (383.46)	0.21 (484.69)	0.36 (385.46)
2016	0.65 (1,112.75)	0.19 (350.74)	0.14 (442.50)	0.28 (371.86)
2017	0.83 (1,161.92)	0.24 (373.37)	0.16 (469.44)	0.34 (366.65)
Total	4.26 (8,821.21)	1.34 (2.846.20)	1.33 (3,610.24)	1.82 (2,892.78)
P-areas (Active Wells)	1,785	1,553	1,465	1,336
All P-areas	2,776	2,519	3,338	2,100

Numbers in parentheses describe the death count.

2.5 emissions. Among all counties, Washington County is mostly affected, with an additional 4.26 deaths between 2010 and 2017. Using a value of statistical life of $7.4 million (2006 dollars) (https://www.epa.gov/environmental-economics/mortality-risk-valuation), the total mortality effect of additional 20.11 deaths can be translated to an economic loss of $148.814 million. This is a lower bound of the total economic loss which is expected to be larger when considering all types of pollution associated with shale gas development.

8 Conclusion and Discussion

The paper estimates use satellite based AOD data to detect the PM pollution from shale gas wells at hyperlocal area. We find significant impact in PM concentration due to the shale gas wells pre-production and production activities in the vicinity of well, with the marginal increase in AOD is higher during pre-production (2.19% relative to the baseline AOD) than during production (1.35% of baseline). Our results suggest that the PM pollution from shale gas wells can travel through wind for up to 10 kilometers, but the pollution disperses and the impact decreases in distance. Accounting for airborne spillovers, fracking increases AOD by 1.27% for the whole sample, and by 5.67% for the subsample of P-areas with a treated well. These overall increases in AOD imply that daily PM concentrations increased by $0.017 mg/m^3$ and $0.062 mg/m^3$, respectively, in the average P-area. Besides, we estimate the impact in mortality caused by the PM emissions from shale gas wells. We find that from 2010 to 2017, there are 671 census block groups across 40 counties that have shale gas wells located in, and there are about 840,000 populations living around shale gas wells. The estimated PM emissions from shale gas wells causes additional 20.11 deaths among these communities.

Currie et al. (2017) and Hill (2018) find that the shale gas development has negative impact in local health outcomes, but there is limited knowledge about through what channels shale gas development affecting health. While there are several studies showing how the shale gas development generates air and water pollution, there is no previous research directly link these pollution to local health outcomes. Our study contribute to the literature by filling this gap. This paper not only provides understandings of how the shale gas wells affect the air quality through PM emissions, but also shows empirical evidence that shale gas wells cause extra mortality in the local communities through generating PM pollution.

Since we only focus on the PM pollution fro shale gas industry, we are not able to estimate the overall externalities. Future researches are needed for investigating the welfare impact of shale gas industry through other channels, such as other air pollutants and water contamination.

A Appendix

A.1 Production Data and Assignment of Treatments

We utilize the information on spud date, plug date, and production period to determine the on-site activities and sources of air pollution on a specific day. We assume a well is subject to pre-production activities from the spud date till the start of production. Assuming the production period is continuous, we define the production period from the first production date to either the last production date or the plug date, depending on which date is later.[15] We use the well production reports to determine the start and end of production for each well. The production reports are available annually before July 2010 , then biannual between July 2010 and December 2014, and eventually every month.

The production reports do not have the specific starting and completion dates. We use the report date and duration to derive the first and last date of the production phase: for each well, we find the earliest production report cycle with positive production, and then define the first production date as the last date in that production report cycle minus production days plus one. The last production date is defined as the first date in the last production report cycle plus production days minus one. The estimated last production date is used to verify the reliability of and to fix the measurement error in the plug date provided in "Oil Gas Locations – Unconventional" data set.

For some wells with limited and incomplete information, we make additional assumptions to define the pre-production phase. For instance, some wells were spudded but not producing so only the start date of the pre-production phase is available, but the end date is unknown. Others were spudded and producing but spud date is missing so only the pre-production end date is available, but the pre-production start date remains unknown. In these cases we use the average pre-production phase length of wells within a 50 km radius to define the pre-production phase. There are 1,698 wells with estimated pre-production phase length.

We do not consider the post-production period in this paper, so all observations after production period end date are removed. In the whole sample, we have 10,479 P-areas under

[15] There are 50 wells with plug date before the last date of production. 47 of them have plug date more than 500 days before production end date. All 50 wells have positive production after their listed plug date. Therefore, we assume these plug dates are incorrectly measured.

treatments. There are 1,846 P-areas with only pre-production treatment, 15 P-areas with only production treatment, and 8,618 P-areas with both treatments. The remaining 8,391 P-areas do not experience any treatment. Our definition of treatments is very consistent with well status as reported in "Oil Gas Locations – Unconventional". Among 10,479 wells with treatments, only 5 of them are labelled as "Proposed But Never Materialized" or "Operator Reported Not Drilled". Based on their production report, they are mistakenly labelled.

A.2 Additional Summary Description

Table A1: Bivariate Correlations Between Variables

	AOD	Pre-production treatment	Production treatment	Pre-production treatment in 0-2 km ring	Pre-production treatment in 2-5 km ring	Pre-production treatment in 5-10 km ring	Production treatment in 0-2 km ring	Production treatment in 2-5 km ring
AOD	1	-	-	-	-	-	-	-
Pre-production treatment	-0.0188	1	-	-	-	-	-	-
Production treatment	-0.0454	-0.0652	1	-	-	-	-	-
Pre-production treatment in 0-2 km ring	-0.0254	0.3075	0.0427	1	-	-	-	-
Pre-production treatment in 2-5 km ring	-0.0485	0.1489	0.1315	0.2564	1	-	-	-
Pre-production treatment in 5-10 km ring	-0.0752	0.1340	0.1655	0.2262	0.4439	1	-	-
Production treatment in 0-2 km ring	-0.0513	0.0248	0.4718	0.0949	0.1987	0.2546	1	-
Production treatmen in 2-5 km ring	-0.0710	0.0701	0.4191	0.1369	0.2608	0.3606	0.5865	1
Production treatmen in 5-10 km ring	-0.0900	0.0777	0.3741	0.1427	0.2801	0.4274	0.4922	0.7381
Density Pre-production (Number of wells, 20 km)	-0.0928	0.2409	0.2037	0.3730	0.6088	0.7789	0.3059	0.4044
Density Production (Number of wells, 20 km)	-0.0928	0.0873	0.4789	0.1630	0.3008	0.4229	0.6113	0.7995
Density Inactive (Number of wells, 20 km)	-0.0592	0.0479	0.3648	0.0684	0.1182	0.1652	0.4376	0.5254
Precipitation (mm)	0.0276	-0.0009	0.0008	-0.0014	-0.0057	-0.0128	-0.0007	-0.0055
Dew Point (Celsius)	0.3704	-0.0046	0.0112	-0.0065	-0.0137	-0.0247	0.0081	0.0012
Temperature (Celsius)	0.3852	-0.0067	0.0039	-0.0082	-0.0147	-0.0239	0.0012	-0.0044
Wind Speed (m/s)	-0.1207	0.0015	0.0001	0.0049	0.0044	0.0046	0.0070	0.0042

	prod_10 in 5-10 km ring	Density Pre-production (Number of wells, 20 km)	Density Production (Number of wells, 20 km)	Density Inactive (Number of wells, 20 km)	Precipitation (mm)	Dew Point (Celsius)	Temperature (Celsius)	Wind Speed (m/s)
AOD	-	-	-	-	-	-	-	-
Pre-production treatment	-	-	-	-	-	-	-	-
Production treatment	-	-	-	-	-	-	-	-
Pre-production treatment in 0-2 km ring	-	-	-	-	-	-	-	-
Pre-production treatment in 2-5 km ring	-	-	-	-	-	-	-	-
Pre-production treatment in 5-10 km ring	-	-	-	-	-	-	-	-
Production treatment in 0-2 km ring	-	-	-	-	-	-	-	-
Production treatment in 2-5 km ring	1	-	-	-	-	-	-	-
Density Pre-production (Number of wells, 20 km) in 5-10 km ring	0.4475	1	-	-	-	-	-	-
Density Production (Number of wells, 20 km)	0.8542	0.5218	1	-	-	-	-	-
Density Inactive (Number of wells, 20 km)	0.5024	0.2064	0.6089	1	-	-	-	-
Precipitation (mm)	0.0110	-0.0141	-0.0114	-0.0041	1	-	-	-
Dew Point (Celsius)	-0.0059	-0.0303	-0.0043	0.0095	0.1916	1	-	-
Temperature (Celsius)	-0.0094	-0.0308	-0.0095	-0.0096	0.1091	0.9490	1	-
Wind Speed (m/s)	0.0025	0.0050	0.0030	0.0143	0.1030	-0.2275	-0.2536	1

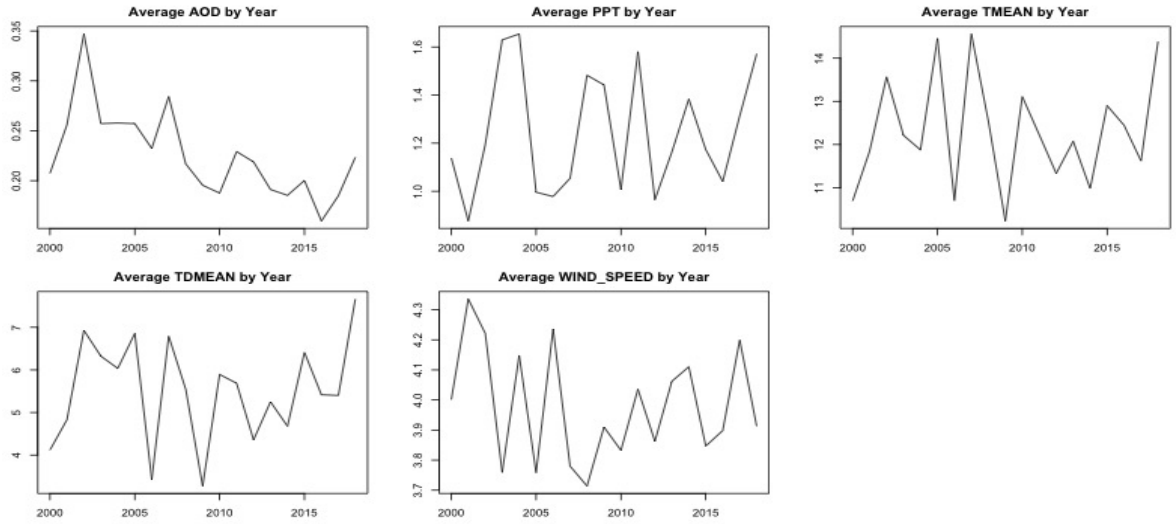

Figure A1: Time Trend – AOD and weather variables

A.3 Common Trend Test

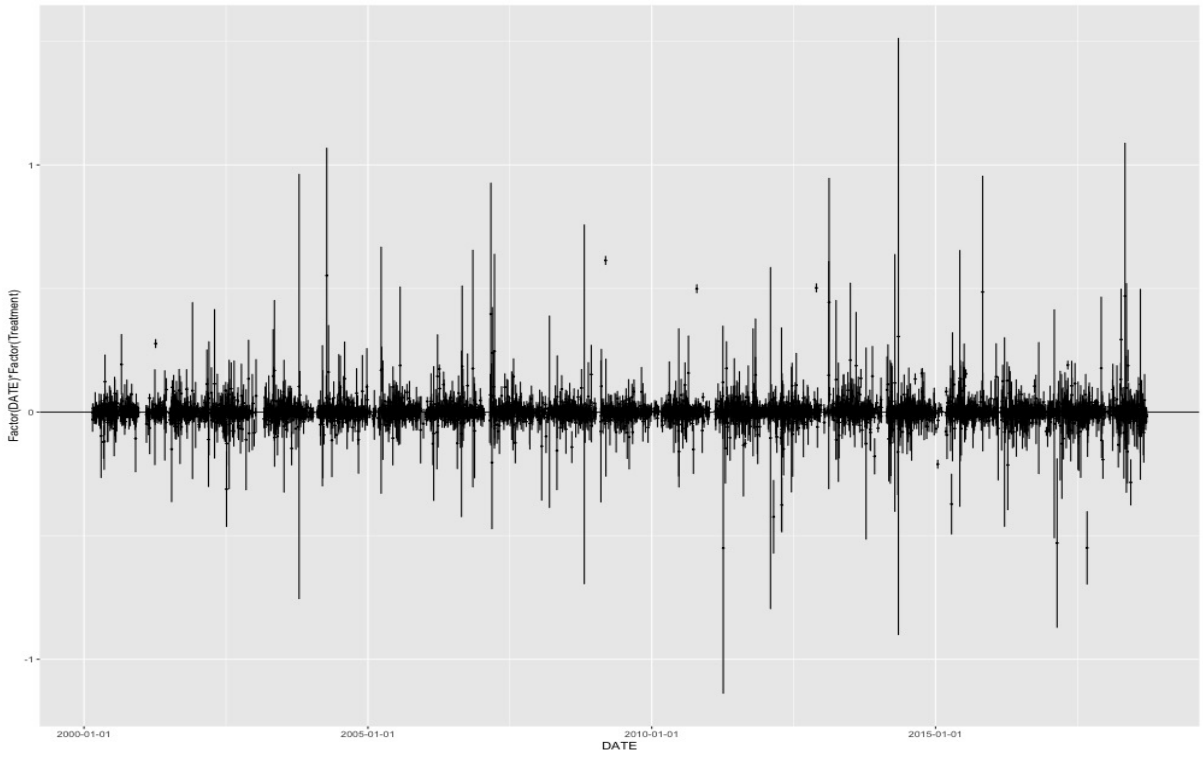

Figure A2: Common Trend Test

Table A2: Common Trend Significance Dates

Significance Level	10%	5%	1%	0.1%	Overall
Number of Significant Dates	1,337	1,028	598	315	4,609
Significant Dates Ratio	29.01%	22.30%	12.97%	6.83%	

A.4 Additional Discussion of Main Results

Figure 2, 3 and 4 show the geographical location of all unconventional wells in PA. We find clusters of unconventional wells in northeast and southwest PA, with a spatial segregation between the treatment and control groups as shown in figure 2 and 3. This can be explained by figure 4, as the distribution of treatment group with both pre-production and production are quite similar to wells with permits issued in 2008-2011, and the distribution of control group is quite similar to wells with permits issued in 2012-2015. These wells belong to the control group because of the late development of the local shale gas industry, and it is possible they will operate in the future.

The coefficients of "Density Pre-production" and "Density Production" are significantly negative, but the coefficient of "Density Inactive" is significantly positive. That is because the density variables have ambiguous effect in the baseline model: First, larger densities means less infrastructure construction and lower AOD. Second, larger densities means more pre-production, production and inactive wells nearby, which increases AOD. Inactive wells may also contribute to AOD because of the cleanup process after the well no longer operated.

Table A3 reports the estimation results of the baseline model and spatial difference-in-differences model. Column (1) and (2) report the results from the baseline model, and column (3) and (4) report the results from spatial difference-in-differences model. Column (1) gives very counter-intuitive results, as pre-production phase does not affect air quality, and production period makes air quality even better. Without controlling density variables, the estimation is heavily biased, because the segregation of treatment group and control group causes the treatments to be non-random in location and time, and makes tow groups incomparable. Column (3) does not include density variables, but by doing spatial difference-in-differences, the coefficients of "Pre-production" and "Production" become significantly positive. However, some coefficients of spatial spillover variables are still counter-intuitive. That is because spatial spillover variables are correlated with number of wells nearby, and partially account for the densities. It also means that density variables are confounders of both treatment dummy variables and spatial spillover variables, and excluding density variables in the regression may downward bias the estimation results. Column (2) and column (4) include density variables in the regression, and the treatment effects of pre-production phase and production period are significantly positive.

Table A3: Main Analysis

AOD	DID		Spatial DID	
	(1)	(2)	(3)	(4)
Own Effects				
Pre-production treatment	0.00028	0.00624***	0.00191***	0.00429***
	(0.00033)	(0.00040)	(0.00033)	(0.00039)
Production treatment	−0.00078***	0.00463***	0.00102***	0.00258***
	(0.00030)	(0.00049)	(0.00032)	(0.00036)
Spillover Effects				
Pre-production treatment from 0–2 km ring			0.00029***	0.00101***
			(0.00008)	(0.00010)
Pre-production treatment from 2-5 km ring			−0.00015***	0.00050***
			(0.00004)	(0.00004)
Pre-production treatment from 5–10 km ring			−0.00066***	0.00008***
			(0.00002)	(0.00002)
Production treatments from 0–2 km ring			0.00037***	0.00066***
			(0.00006)	(0.00008)
Production treatments from 2–5 km ring			0.00009***	0.00026***
			(0.00002)	(0.00003)
Production treatments from 5–10 km ring			−0.00035***	0.00002**
			(0.00001)	(0.00001)
Covariates				
Number of Pre-production treatment wells in 0-20km		−0.00013***		−0.00016***
		(0.00000)		(0.00000)
Number of production wells in 0-20km		−0.00008***		−0.00009***
		(0.00000)		(0.00000)
Number of inactive wells in 0-20km		0.00023***		0.00022***
		(0.00001)		(0.00001)
Daily precipitation	0.00018***	0.00020***	0.00018***	0.00020***
	(0.00003)	(0.00003)	(0.00003)	(0.00003)
Daily mean dew point	0.01319***	0.01247***	0.01300***	0.01245***
	(0.00012)	(0.00011)	(0.00012)	(0.00011)
Daily mean temperature	−0.00339***	−0.00286***	−0.00315***	−0.00287***
	(0.00009)	(0.00009)	(0.00009)	(0.00009)
Wind_Speed	−0.00155***	−0.00157***	−0.00154***	−0.00158***
	(0.00008)	(0.00008)	(0.00008)	(0.00008)
Well FE	Y	Y	Y	Y
Date FE	Y	Y	Y	Y
Cluster	PAD	PAD	PAD	PAD
Observations	31,531,987	31,531,987	31,531,987	31,531,987
R^2	0.76073	0.76259	0.76122	0.76268
Adjusted R^2	0.76054	0.76240	0.76103	0.76248
Residual Std. Error	0.12761 (df = 31506614)	0.12712 (df = 31506611)	0.12748 (df = 31506608)	0.12709 (df = 31506605)

Wind_speed is the daily wind speed at the location of centroid well of each P-area;
Standard errors are clustered by well pad;
Standard errors: ***$p < .01$,** $p < .05$,* $p < .1$;

A.5 Full Results of Robustness Check

Table A4: Sensitivity Analysis 1 – Using Treatment Group Only

AOD	Baseline Model		Spatial Diff-in-diff Model	
	(1)	(2)	(3)	(4)
Pre-production treatmen	0.00058*	0.00651***	0.00200***	0.00475***
	(0.00033)	(0.00040)	(0.00035)	(0.00040)
Production	−0.00069*	0.00488***	0.00070*	0.00281***
	(0.00038)	(0.00060)	(0.00042)	(0.00059)
Pre-production_2			0.00019**	0.00086***
			(0.00009)	(0.00010)
Pre-production_5			−0.00015***	0.00048***
			(0.00004)	(0.00004)
Pre-production_10			−0.00064***	0.00008***
			(0.00002)	(0.00002)
Production_2			0.00032***	0.00060***
			(0.00007)	(0.00009)
Production_5			0.00008***	0.00025***
			(0.00003)	(0.00003)
Production_10			−0.00034***	0.00003**
			(0.00001)	(0.00001)
Density Pre-production		−0.00013***		−0.00016***
		(0.00000)		(0.00000)
Density Production		−0.00009***		−0.00010***
		(0.00000)		(0.00000)
Density Inactive		0.00021***		0.00021***
		(0.00001)		(0.00001)
Daily Precipitation	0.00016***	0.00019***	0.00016***	0.00019***
	(0.00003)	(0.00003)	(0.00003)	(0.00003)
Daily mean dew point	0.01374***	0.01296***	0.01355***	0.01294***
	(0.00014)	(0.00014)	(0.00014)	(0.00014)
Daily mean temperature	−0.00342***	−0.00284***	−0.00318***	−0.00285***
	(0.00011)	(0.00011)	(0.00011)	(0.00011)
Wind_Speed	−0.00181***	−0.00185***	−0.00180***	−0.00186***
	(0.00008)	(0.00008)	(0.00009)	(0.00008)
Well FE	Y	Y	Y	Y
Date FE	Y	Y	Y	Y
Cluster	PAD	PAD	PAD	PAD
Observations	17,506,147	17,506,147	17,506,147	17,506,147
R^2	0.76242	0.76444	0.76294	0.76454
Adjusted R^2	0.76221	0.76423	0.76272	0.76432
Residual Std. Error	0.12672 (df = 17490026)	0.12618 (df = 17490023)	0.12658 (df = 17490020)	0.12615 (df = 17490017)

Standard errors: *p<0.1; **p<0.05; ***p<0.01

Table A5: Sensitivity Analysis 2 – Standard Diff-in-Diff Using Matched Samples

AOD	Matched sample 1	Matched sample 2	Matched sample 1	Matched sample 2
	(1)	(2)	(3)	(4)
Pre-production	0.00050	0.00047	0.00609***	0.00624***
	(0.00032)	(0.00032)	(0.00039)	(0.00039)
Production	−0.00051	−0.00057*	0.00449***	0.00475***
	(0.00031)	(0.00032)	(0.00051)	(0.00051)
Density Pre-production			−0.00013***	−0.00013***
			(0.00000)	(0.00000)
Density Production			−0.00009***	−0.00009***
			(0.00000)	(0.00000)
Density Inactive			0.00021***	0.00021***
			(0.00001)	(0.00001)
Daily precipitation	0.00018***	0.00017***	0.00020***	0.00019***
	(0.00003)	(0.00003)	(0.00003)	(0.00003)
Daily mean dew point	0.01347***	0.01347***	0.01271***	0.01270***
	(0.00013)	(0.00014)	(0.00012)	(0.00013)
Daily temperature	−0.00341***	−0.00344***	−0.00284***	−0.00286***
	(0.00010)	(0.00010)	(0.00010)	(0.00010)
Wind_Speed	−0.00173***	−0.00174***	−0.00176***	−0.00177***
	(0.00008)	(0.00008)	(0.00008)	(0.00008)
Well FE	Y	Y	Y	Y
Date FE	Y	Y	Y	Y
Cluster	PAD	PAD	PAD	PAD
Observations	21,949,389	21,583,079	21,949,389	21,583,079
R^2	0.76163	0.76201	0.76361	0.76400
Adjusted R^2	0.76142	0.76180	0.76340	0.76379
Residual Std. Error	0.12710 (df = 21930365)	0.12700 (df = 21564321)	0.12657 (df = 21930362)	0.12647 (df = 21564318)

The matched subsample 1 is matched by distance, permit year and permit month.
The matched subsample 2 is matched by distance, permit year and county.
Standard errors: *p<0.1; **p<0.05; ***p<0.01

Table A6: Sensitivity Analysis 3 – Spatial Diff-in-Diff Using Matched Samples

AOD	Matched sample 1	Matched sample 2	Matched sample 1	Matched sample 2
	(1)	(2)	(3)	(4)
Pre-production	0.00191***	0.00192***	0.00436***	0.00452***
	(0.00033)	(0.00033)	(0.00038)	(0.00038)
Production	0.00088***	0.00092***	0.00262***	0.00291***
	(0.00034)	(0.00034)	(0.00048)	(0.00049)
Pre-production_2	0.00022**	0.00021**	0.00093***	0.00093***
	(0.00009)	(0.00009)	(0.00010)	(0.00010)
Pre-production_5	−0.00015***	−0.00015***	0.00043***	0.00048***
	(0.00004)	(0.00004)	(0.00004)	(0.00004)
Pre-production_10	−0.00065***	−0.00065***	0.00008***	0.00008***
	(0.00002)	(0.00002)	(0.00002)	(0.00002)
Production_2	0.00033***	0.00031***	0.00061***	0.00060***
	(0.00007)	(0.00006)	(0.00008)	(0.00009)
Production_5	0.00008***	0.00009***	0.00026***	0.00027***
	(0.00002)	(0.00002)	(0.00003)	(0.00003)
Production_10	−0.00035***	−0.00035***	0.00002**	0.00002**
	(0.00001)	(0.00001)	(0.00001)	(0.00001)
Density Pre-production			−0.00016***	−0.00016***
			(0.00000)	(0.00000)
Density Production			−0.00009***	−0.00009***
			(0.00000)	(0.00000)
Density Inactive			0.00021***	0.00020***
			(0.00001)	(0.00001)
Daily precipitation	0.00018***	0.00017***	0.00020***	0.00019***
	(0.00003)	(0.00003)	(0.00003)	(0.00003)
Daily mean dew point	0.01328***	0.01328***	0.01269***	0.01268***
	(0.00013)	(0.00013)	(0.00013)	(0.00013)
Daily mean temperature	−0.00316***	−0.00320***	−0.00285***	−0.00288***
	(0.00010)	(0.00010)	(0.00010)	(0.00010)
Wind_Speed	−0.00171***	−0.00173***	−0.00177***	−0.00178***
	(0.00008)	(0.00008)	(0.00008)	(0.00008)
Well FE	Y	Y	Y	Y
Date FE	Y	Y	Y	Y
Cluster	PAD	PAD	PAD	PAD
Observations	21,949,389	21,583,079	21,949,389	21,583,079
R^2	0.76214	0.76252	0.76370	0.76409
Adjusted R^2	0.76193	0.76231	0.76350	0.76389
Residual Std. Error	0.12697 (df = 21930359)	0.12686 (df = 21564315)	0.12655 (df = 21930356)	0.12644 (df = 21564312)

The matched subsample 1 is matched by distance, permit year and permit month.
The matched subsample 2 is matched by distance, permit year and county.
*p<0.1; **p<0.05; ***p<0.01

Table A7: Robustness check: spatial DID using longer pre-production windows

	Window 1	Window 2	Window 1	Window 2
window	0.00626***	0.00620***	0.00434***	0.00433***
	(0.00040)	(0.00039)	(0.00039)	(0.00038)
prod	0.00466***	0.00470***	0.00260***	0.00264***
	(0.00049)	(0.00049)	(0.00046)	(0.00046)
window_2			0.00101***	0.00101***
			(0.00010)	(0.00010)
window_5			0.00050***	0.00050***
			(0.00004)	(0.00004)
window_10			0.00008***	0.00008***
			(0.00002)	(0.00002)
prod_2			0.00066***	0.00066***
			(0.00008)	(0.00008)
prod_5			0.00026***	0.00026***
			(0.00003)	(0.00003)
prod_10			0.00002**	0.00002**
			(0.00001)	(0.00001)
Treatment_window_Count	−0.00013***	−0.00013***	−0.00016***	−0.00016***
	(0.00000)	(0.00000)	(0.00000)	(0.00000)
Treatment_prod_count	−0.00008***	−0.00008***	−0.00009***	−0.00009***
	(0.00000)	(0.00000)	(0.00000)	(0.00000)
Plug_Count	0.00023***	0.00023***	0.00022***	0.00022***
	(0.00001)	(0.00001)	(0.00001)	(0.00001)
PPT	0.00020***	0.00020***	0.00020***	0.00020***
	(0.00003)	(0.00003)	(0.00003)	(0.00003)
TDMEAN	0.01247***	0.01247***	0.01245***	0.01245***
	(0.00011)	(0.00011)	(0.00011)	(0.00011)
TMEAN	−0.00286***	−0.00286***	−0.00287***	−0.00287***
	(0.00009)	(0.00009)	(0.00009)	(0.00009)
Wind_Speed	−0.00157***	−0.00157***	−0.00158***	−0.00158***
	(0.00008)	(0.00008)	(0.00008)	(0.00008)
Well and Date FEs	Y	Y	Y	Y
Observations	31,531,987	31,531,987	31,531,987	31,531,987
R^2	0.76259	0.76259	0.76268	0.76268
Adjusted R^2	0.76240	0.76240	0.76248	0.76248
Residual Std. Error	0.12712	0.12712	0.12709	0.12709
Residual Std. Error	(df = 31506611)	(df = 31506611)	(df = 31506605)	(df = 31506605)

Note: Window 1 start from 7 days before spud date, Window 2 starts from 30 days before spud date.

Table A8: Robustness check: falsification tests

AOD	Baseline Model		Spatial Diff-in-diff Model	
	(1)	(2)	(3)	(4)
Placebo Treatment	0.00019	−-0.00015	0.00036	0.00008
	(0.00034)	(0.00034)	(0.00033)	(0.00034)
Pre-production_2			0.00120***	0.00119***
			(0.00012)	(0.00012)
Pre-production_5			0.00055***	0.00055***
			(0.00005)	(0.00005)
Pre-production_10			0.00013***	0.00013***
			(0.00002)	(0.00002)
Production_2			0.00070***	0.00070***
			(0.00010)	(0.00010)
Production_5			0.00029***	0.00029***
			(0.00004)	(0.00004)
Production_10			0.00002*	0.00002*
			(0.00001)	(0.00001)
Density Pre-production	−0.00015***	−0.00015***	−0.00017***	−0.00017***
	(0.00000)	(0.00000)	(0.00000)	(0.00000)
Density Production	−0.00008***	−0.00008***	−0.00008***	−0.00009***
	(0.00000)	(0.00001)	(0.00000)	(0.00000)
Density Inactive	0.00023***	0.00023***	0.00022***	0.00022***
	(0.00001)	(0.00001)	(0.00001)	(0.00001)
Daily precipitation	0.00029***	0.00029***	0.00029***	0.00029***
	(0.00003)	(0.00003)	(0.00003)	(0.00003)
Daily mean dew point	0.01272***	0.01272***	0.01270***	0.01270***
	(0.00012)	(0.00012)	(0.00012)	(0.00012)
Daily mean temperature	−0.00321***	−0.00321***	−0.00321***	−0.00321***
	(0.00010)	(0.00010)	(0.00010)	(0.00010)
Wind_Speed	−0.00155***	−0.00155***	−0.00157***	−0.00157***
	(0.00008)	(0.00008)	(0.00008)	(0.00008)
Well FE	Y	Y	Y	Y
Date FE	Y	Y	Y	Y
Cluster	PAD	PAD	PAD	PAD
Observations	26,920,567	26,920,567	26,920,567	26,920,567
R^2	0.76519	0.76519	0.76526	0.76526
Adjusted R^2	0.76497	0.76497	0.76504	0.76504
Residual Std. Error	0.12952	0.12952	0.12950	0.12950
Residual Std. Error	(df = 26895198)	(df = 26895198)	(df = 26895192)	(df = 26895192)

Note: Standard errors are clustered by wells pad.

A.6 Additional maps of wells

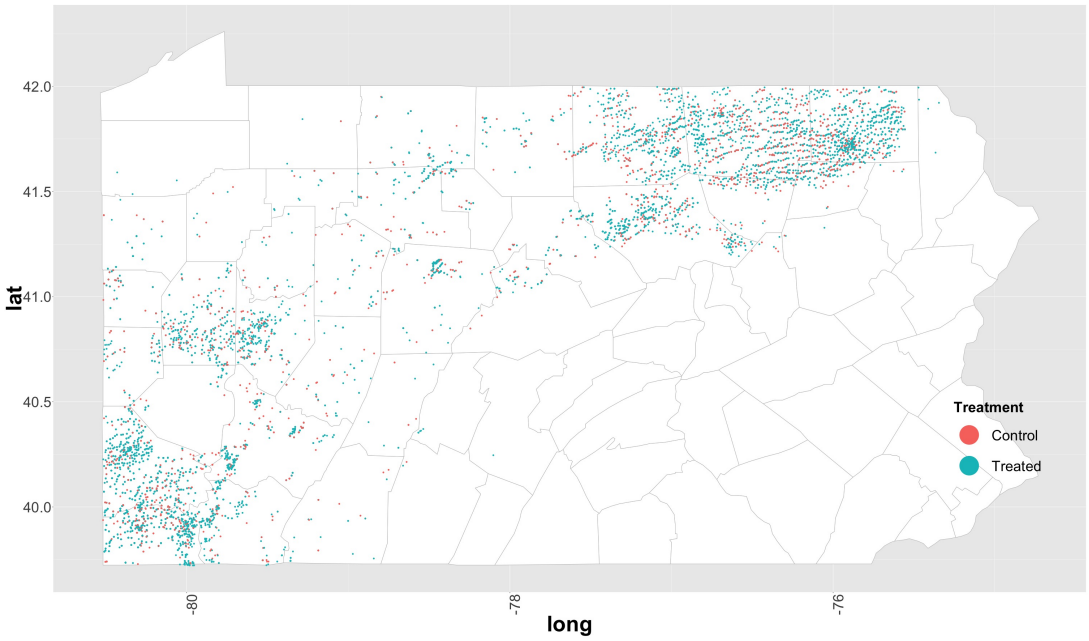

Figure A3: Matched sample 1 – wells matched by distance, permit year, and permit month

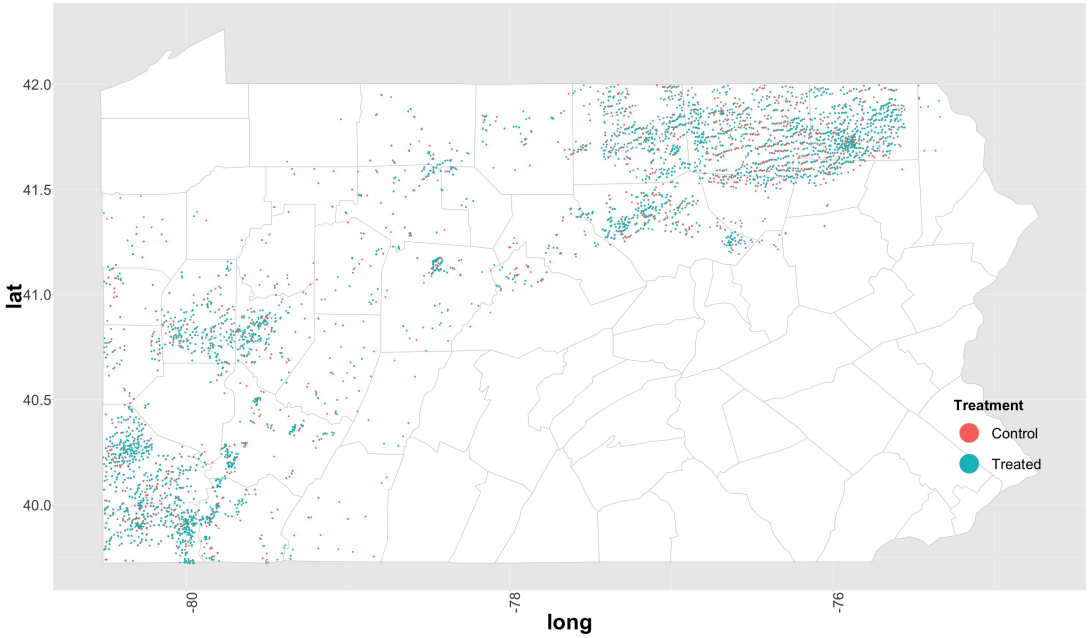

Figure A4: Matched sample 2 – wells matched by distance, permit year, and county

A.7 Convert AOD to PM 2.5

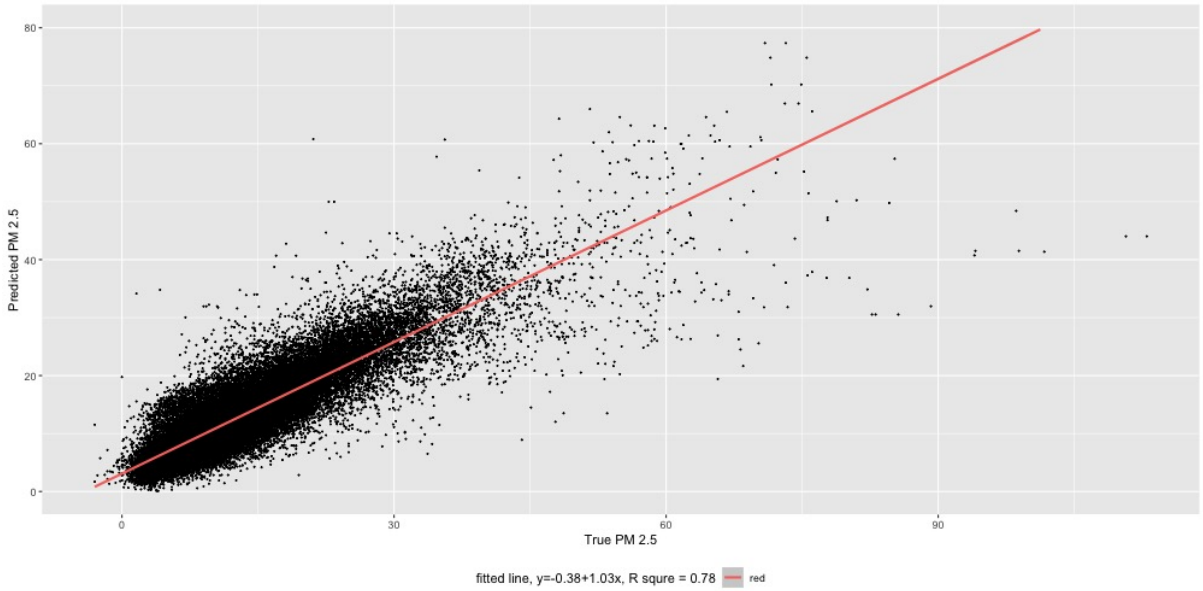

Figure A5: PM 2.5 Prediction, PM 2.5 Monitors in Pennsylvania

A.8 Cox proportional-hazard model

Estimating the Cox proportional-hazard model yields the relative mortality rate (RR), which is the ratio of mortality rates under different pollution concentration.

$$RR = \frac{\lambda(X, PM'_{2.5})}{\lambda(X, PM''_{2.5})} = exp(\hat{\gamma}(PM'_{2.5} - PM''_{2.5})). \tag{10}$$

X is a vector of covariates related with mortality, $\lambda(X, PM'_{2.5})$ and $\lambda(X, PM''_{2.5})$ are mortality rates under two different PM 2.5 concentrations $PM'_{2.5}$ and $PM''_{2.5}$. $\hat{\gamma}$ is the estimated coefficient of RR, which indicates the mortality impact by changing PM 2.5 concentration from $PM'_{2.5}$ to $PM''_{2.5}$.

References

Allen, D. T., Torres, V. M., Thomas, J., Sullivan, D. W., Harrison, M., Hendler, A., Herndon, S. C., Kolb, C. E., Fraser, M. P., Hill, A. D., et al. (2014). Measurements of methane emissions at natural gas production sites in the united states. *Proceedings of the National Academy of Sciences*, 110(44):17768–17773.

Athey, S. and Imbens, G. W. (2018). Design-based analysis in difference-in-differences settings with staggered adoption. *NBER*, working paper.

Atkinson, R. W., Kang, S., Anderson, H. R., Mills, I. C., and Walton, H. A. (2014). Epidemiological time series studies of pm2.5 and daily mortality and hospital admissions: a systematic review and meta-analysis. *Respiratory Epidemiology*, 69:650–662.

Currie, J., Greenstone, M., and Meckel, K. (2017). Hydraulic fracturing and infant health: New evidence from pennsylvania. *Science Advances*, 3(12).

Delgado, M. S. and Florax, R. J. (2015). Difference-in-differences techniques for spatial data: Local autocorrelation and spatial interaction. *Economics Letters*, 137:123–126.

Donkelaar, A. V., Martin, R. V., Brauer, M., Hsu, N. C., Kahn, R. A., Levy, R. C., Lyapustin, A., Sayer, A. M., and Winker, D. M. (2016). Global estimates of fine particulate matter using a combined geophysical-statistical method with information from satellites, models, and monitors. *Environmental Science and Technology*, 50:3762–3772.

EIA Website (2019). Shale gas production. https://www.eia.gov/dnav/ng/ng_prod_shalegas_s1_a.htm, Accessed in: March 2020.

Field, R. A., Soltis, J., and Murphy, S. (2014). Air quality concerns of unconventional oil and natural gas production. *Environmental Science Processes and Impact*, 16:954–969.

Foster, A., Gutierrez, E., and Kumar, N. (2009). Voluntary compliance, pollution levels, and infant mortality in mexico. *American Economic Review*, 99(2):191–197.

Fowlie, M., Rubin, E. A., and Walker, R. (2019). Bringing satellite-based air quality estimates down to earth. *AEA Papers and Proceedings*, 109(1):283–288.

Goodman-Bacon, A. (2018). Difference-in-differences with variation in treatment timing. *NBER*, working paper.

Graham, J., Irving, J., Tang, X., Sellers, S., Crisp, J., Horwitz, D., Muehlenbachs, L., Krupnick, A., and Carey, D. (2015). Increased traffic accident rates associated with shale gas drilling in pennsylvania. *Accident Analysis and Prevention*, 74:203–209.

Heo, J. B., Hopke, P. K., and Yi, S. (2009). Source apportionment of pm2.5 in seoul, korea. *Atmospheric Chemistry and Physics*, 9:4957–4971.

Hill, E. and Ma, L. (2017). Shale gas development and drinking water quality. *American Economic Review*, 107(5):522–525.

Hill, E. L. (2018). Shale gas development and infant health: Evidence from pennsylvania. *Journal of Health Economics*, 61:134–150.

Huang, R.-J., Zhang, Y., Bozzetti, C., Ho, K.-F., Cao, J.-J., Han, Y., Daellenbach, K. R., Slowik, J. G., Platt, S. M., Canonaco, F., Zotter, P., Wolf, R., Pieber, S. M., Bruns, E. A., Crippa, M., Ciarelli, G., Piazzalunga, A., Schwikowski, M., Abbaszade, G., Schnelle-Kreis, J., Zimmermann, R., An, Z., Szidat, S., Baltensperger, U., Haddad, I. E., and 1, A. S. H. P. (2014). High secondary aerosol contribution to particulate pollution during haze events in china. *Nature*, 514:218–222.

Jackson, R. B., Vengosh, A., Darrah, T. H., Warner, N., Down, A., Poreda, R. J., Osborn, S. G., Zhao, K., and Karr, J. D. (2013). Increased stray gas abundance in a subset of drinking water wells near marcellus shale gas extraction. *Proceedings of the National Academy of Sciences*, 110(28):11250–11255.

Krewski, D., Jerrett, M., Burnett, R. T., Ma, R., Hughes, E., Shi, Y., Turner, M. C., Pope III, C. A., Thurston, G., Calle, E. E., and Thun et al, M. J. (2009). Extended follow-up and spatial analysis of the american cancer society study linking particulate air pollution and mortality. *Health Effects Institute Boston, MA*.

Kumar, N., Chu, A., and Foster, A. (2007). An empirical relationship between pm2.5 and aerosol optical depth in delhi metropolitan. *Atmospheric Environment*, 41:4492–4503.

Larsen, B., Gilardoni, S., Stenström, K., Niedzialek, J., Jimenez, J., and Belis, C. (2012). Sources for pm air pollution in the po plain, italy: Ii. probabilistic uncertainty characterization and sensitivity analysis of secondary and primary sources. *Atmospheric Environment*, 50:203–213.

Lee, H. J., Liu, Y., Coull, B. A., Schwartz, J., and Koutrakis, P. (2011). A novel calibration approach of modis aod data to predict $pm_{2.5}$ concentrations. *Atmospheric Chemistry and Physics*, 11(15):7991–8002.

Lepeule, J., Laden, F., Dockery, D., and Schwartz, J. (2012). Chronic exposure to fine particles and mortality: an extended follow-up of the harvard six cities study from 1974 to 2009. *Environmental health perspectives*, 120(7):965.

Lewandowski, M., Jaoui, M., Offenberg, J. H., Kleindienst, T. E., Edney, E. O., Sheesley, R. J., and Schauer, J. J. (2008). Primary and secondary contributions to ambient pm in the midwestern united states. *Environmental Science Technology*, 42(9):3303–3309.

Litovitz, A., Curtright, A., Abramzon, S., Burger, N., and Samaras, C. (2013). Estimation of regional air-quality damages from marcellus shale natural gas extraction in pennsylvania. *Environmental Research Letters*, 8(1):014017.

Liu, Y., Park, R. J., Jacob, D. J., Li, Q., Kilaru, V., and Sarnat, J. A. (2004). Mapping annual mean ground-level pm 2.5 concentrations using multiangle imaging spectroradiometer aerosol optical thickness over the contiguous united states. *Journal of Geophysical Research*, 109(D12):D22206.

Muehlenbachs, L., Spiller, E., and Timmins, C. (2015). The housing market impacts of shale gas development. *American Economic Review*, 105(12):3633–3659.

Newell, R. G. and Raimi, D. (2014). Implications of shale gas development for climate change. *Environmental Science & Technology*, 48(15):8360–8368.

Olmstead, S. M., Muehlenbachs, L. A., Shih, J.-S., Chu, Z., and Krupnick, A. J. (2013). Shale gas development impacts on surface water quality in pennsylvania. *Proceedings of the National Academy of Sciences*, 110(13):4962.

Osborn, S., Vengosh, A., Warner, N., and Jackson, R. (2011). Methane contamination of drinking water accompanying gas well drilling and hydraulic fracturing. *Proceedings of the National Academy of Sciences*, 108(20):8172–8176.

PA DEP Web (2012). All permits issued & wells drilled. http://files.dep.state.pa.us/OilGas/BOGM/BOGMPortalFiles/OilGasReports/2012/2009Wellspermitte-drilled.pdf, Accessed in: March 2020.

PSU Web (2009). Depth of marcellus shale base. http://www.marcellus.psu.edu/resources/images/marcellus-depth.gif, Accessed in: Mar. 2020.

Remer, L. A., Mattoo, S., Levy, R. C., and Munchak, L. A. (2005). Modis 3km aerosol product: algorithm and global perspective. *Journal of the Atmospheric Sciences*, 62(4):947–973.

Roy, A. A., Adams, P. J., and Robinson, A. L. (2014). Air pollutant emissions from the development, production, and processing of marcellus shale natural gas. *Journal of the Air and Waste Management Association*, 64(1):19–37.

Sarigiannis, D., Handakas, E., Kermenidou, M., Zarkadas, I., Gotti, A., Charisiadis, P., Makris, K., Manousakas, M., Eleftheriadis, K., and Karakitsios, S. (2017). Monitoring of air pollution levels related to charilaos trikoupis bridge. *Science of The Total Environment*, 609:1451 – 1463.

Sieminski, A. (2014). Implications of the u.s. shale revolution. *EIA US-Canada Energy Summit, Chicago*.

Srebotnjak, T. and Rotkin-Ellman, M. (2014). Fracking fumes: Air pollution from hydraulic fracturing threatens public health and communities. *NRDC Issue BRIEF*, 14:10–a.

Streets, D. G., Canty, T., R., G., Carmichael, de Foy, B., Dickerson, R. R., Duncan, B. N., Edwards, D. P., Haynes, J. A., Henze, D. K., Houyoux, M. R., Jacob, D. J., Krotkov, N. A., Lamsal, L. N., Liu, Y., Lu, Z., Martin, R. V., Pfister, G. G., Pinderm, R. W., Salawitch, R. J., and Wecht, K. J. (2013). Emissions estimation from satellite retrievals: A review of current capability. *Atmospheric Environment*, 77:1011–1042.

Sullivan, D. M. and Krupnick, A. (2019). Using satellite data to fill the gaps in the us air pollution monitoring network. *RFF*, working paper.

Zou, E. (2019). Unwatched pollution: The effect of intermittent monitoring on air quality. *American Economic Review*, forthcoming.